DISSERTATION ZUR ERLANGUNG DES DOKTORGRADES

DER FAKULTÄT FÜR CHEMIE UND PHARMAZIE
DER LUDWIG-MAXIMILIANS-UNIVERSITÄT

THE V-ATPASE INHIBITOR ARCHAZOLID - IMPACT ON ANOIKIS RESISTANCE IN METASTATIC CANCER CELLS

Christina Maria Schempp
aus
Stuttgart

2014

E R K L Ä R U N G

Diese Dissertation wurde im Sinne von § 7 der Promotionsordnung vom 28. November 2011 von Frau Prof. Dr. Angelika M. Vollmar betreut.

E I D E S T A T T L I C H E V E R S I C H E R U N G

Diese Dissertation wurde eigenständig und ohne unerlaubte Hilfsmittel erarbeitet.

München, den _____

_____

(Christina Maria Schempp)

Dissertation eingereicht am: 25.02.2014

1. Gutachter: Prof. Dr. Angelika M. Vollmar

2. Gutachter: Prof. Dr. Stefan Zahler

Mündliche Prüfung am: 28.03.2014

MEINER MUTTER

SUMMARY

Fighting metastasis is a major challenge in cancer therapy and novel therapeutic targets and drugs are highly appreciated. Resistance of invasive cells to anoikis, a particular type of apoptosis induced by loss of cell-extracellular matrix (ECM) contact, is a major prerequisite for their metastatic spread. Inducing anoikis in metastatic cancer cells is therefore a promising therapeutic approach.

The vacuolar H^+-ATPase (V-ATPase), a proton pump located at the membrane of acidic organelles, has recently come to focus as an anti-metastatic cancer target. As V-ATPase inhibitors have shown to prevent invasion of tumor cells and are able to induce apoptosis we proposed that V-ATPase inhibition induces anoikis related pathways in invasive cancer cells.

In this study the V-ATPase inhibitor archazolid A was used to investigate the mechanism of anoikis induction in various metastatic cancer cells (T24, MDA-MB-231, 4T1, 5637). Therefore, cells were forced to stay in a detached status to mimic loss of cell-ECM engagement following treatment with archazolid.

Indeed, anoikis induction by archazolid was characterized by decreased expression of the caspase-8 inhibitor c-FLIP and caspase-8 activation, thus triggering the extrinsic apoptotic pathway. Interestingly, active integrin β1, which is known to play a major role in anoikis induction and resistance, is reduced on the cell surface of archazolid treated cells. Furthermore, a diminished phosphorylation of the integrin downstream target focal adhesion kinase could be demonstrated. The intrinsic apoptotic pathway was initiated by the pro-apoptotic protein BIM, increasing early after treatment. BIM activates cytochrome C release from the mitochondria consequently leading to cell death and is described as one major inducer of anoikis in non-malignant and anoikis sensitive cancer cells.

Of note, we observed that archazolid also induces mechanisms opposing anoikis such as proteasomal degradation of BIM mediated by the pro-survival kinases ERK, c-Src and especially Akt at later time points. Moreover, induction of reactive oxygen species (ROS) influences BIM removal as well, as moderate levels of ROS have second messenger properties amplifying cell survival signals. Thus, to antagonize these anoikis escape strategies a combination of archazolid with proteasome or ROS inhibitors amplified cancer cell death synergistically.

Most importantly, intravenous injection of archazolid treated 4T1-Luc2 mouse breast cancer cells in BALB/cByJRj mice resulted in reduced lung metastases *in vivo*.

To summarize this work we propose archazolid as a very potent drug in inducing anoikis pathways in metastatic cancer cells even though having learned that detachment together with treatment triggers multiple resistance mechanisms opposing cell death.

Hence, V-ATPase inhibition is not only an interesting option to reduce cancer metastasis but also to better understand anoikis resistance and to find choices to fight against it.

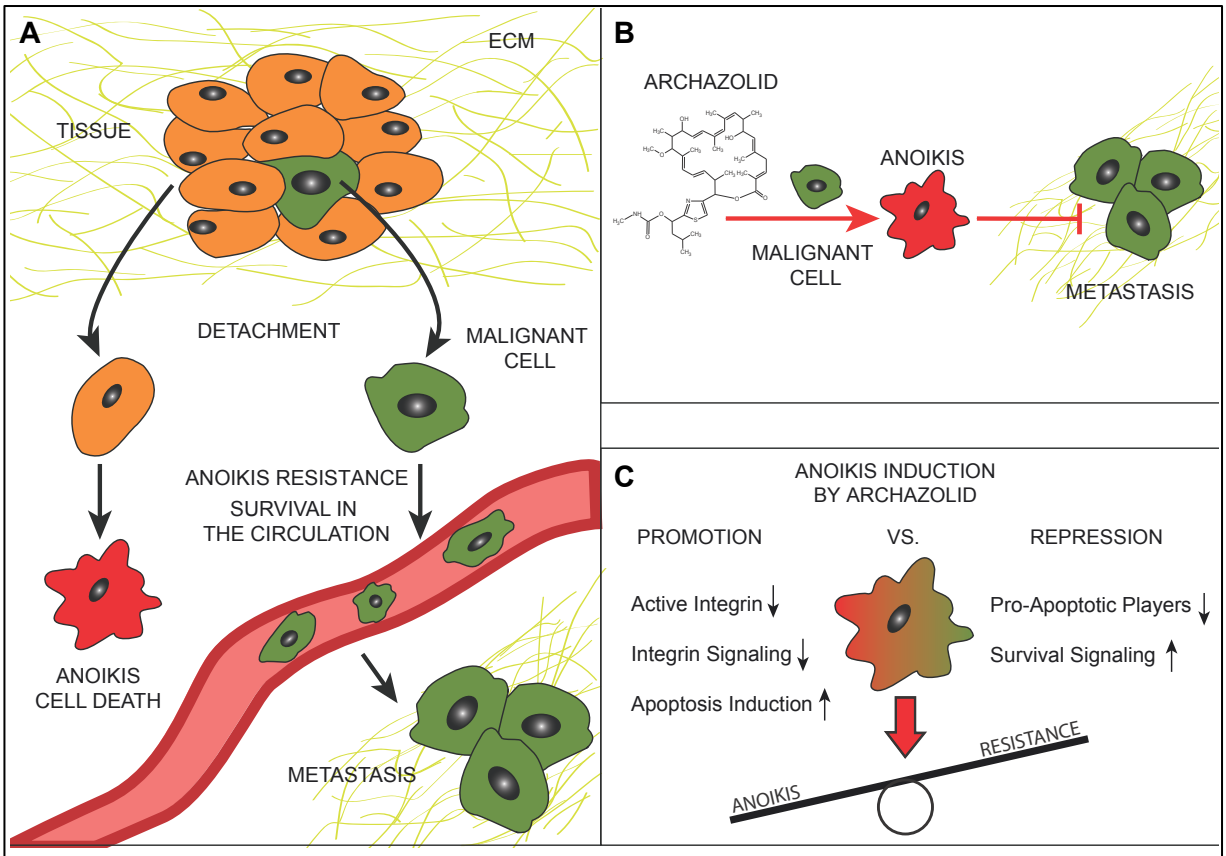

Figure 1: Anoikis, anoikis resistance and actions of archazolid

A: Detachment induces cell death (anoikis) in non-malignant cells preventing a dysplastic growth of tissue cells in other locations, important for tissue homeostasis. Metastatic cancer cells develop anoikis resistance to survive in the circulation, which is a prerequisite for tumor metastasis.

B: Archazolid induces anoikis in malignant cells, thus preventing metastasis.

C: Archazolid treatment promotes anoikis by downregulation of active integrin on the cell surface, attenuating integrin signaling and inducing apoptosis. This is accompanied by mechanisms opposing anoikis induction like activation of certain survival signals and repression of apoptotic proteins. Nevertheless, anoikis signals outweigh anoikis repressing signals induced by archazolid treatment finally leading to cell death and reduced metastasis *in vivo*.

TABLE OF CONTENTS

INTRODUCTION

1 INTRODUCTION

1.1 The V-ATPase as Cancer Target

1.1.1 Physiological Function and Structure

Vacuolar H^+-ATPases (V-ATPases) are ATP-dependent proton pumps ubiquitously expressed, regulating the pH in endomembrane systems like endosomes, lysosomes, the Golgi apparatus and secretory vesicles thus affecting receptor-mediated endocytosis, protein degradation, membrane fusion and intracellular trafficking (1). Some specialized cell types even express the V-ATPase on their plasma membrane for acidification of the extracellular space needed e.g. for renal acidification or bone resorption (2,3).

The V-ATPase is a large multisubunit complex (Figure 2) basically working by a rotary mechanism, organized in two major domains (V1 and V0). The V1 domain is located at the periphery of the cytoplasmic membrane side responsible for ATP hydrolysis providing energy for the rotary movement. It consists of eight different subunits (A-H). The central hexametric ring consists of three AB heterodimers building the catalytic site for ATP hydrolysis. Subunits C-H form peripheral and central stalks connecting V1 and V0. The central stalk functions as rotor transferring the energy of the hydrolysis in a rotation of a ring of proteolipid subunits in the V0 domain.

The V0 domain is embedded in the membrane conducting the proton translocation from the cytoplasm to the lumen. It consists of six different subunits (a, d, e, c, c´, c´´). The protons are translocated by two hemi-channels in the a-subunit and the rotation of the proteolipid ring of four c, c´and c´´ subunits. Each proteolipid contains a buried glutamate residue responsible for proton binding and transportation. Protons can enter the first hemi-channel in the a-subunit at the cytoplasmic side of the membrane and subsequently bind the glutamate residue of one c-subunit. The proteolipid ring rotates, driven by ATP hydrolysis in the V1 domain thereby transporting the H^+ to the second hemi-channel releasing the proton to the lumen (2). Although the V-ATPase is structurally and mechanically related to the F_1F_0 ATPase (F-ATPase) of mitochondria the V-ATPase cannot synthesize ATP from ADP and phosphate (4,5).

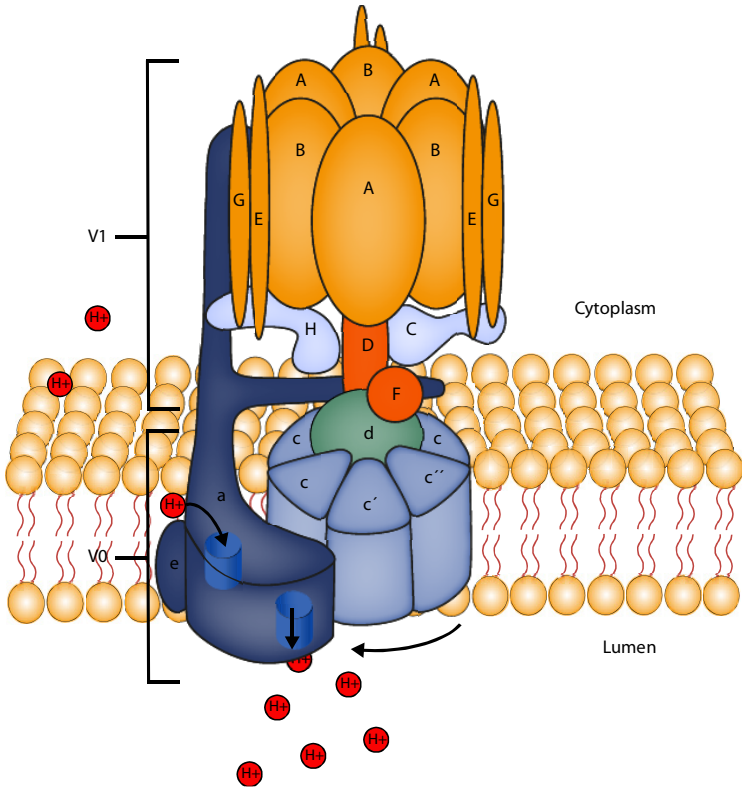

Figure 2: Structure of the vacuolar H⁺-ATPase
The V-ATPase is a proton pump responsible for the acidification of intracellular compartments. It is a multisubunit complex organized in two major domains (V1 and V0). The V1 domain is responsible for ATP hydrolysis to drive the rotary mechanism that translocates the protons in the V0 domain from the cytoplasm to the lumen. Protons can enter a hemi-channel in the a-subunit in the V0 domain and bind a glutamate residue in one of the c-subunits. By the rotation of the c-subunit ring, driven by ATP hydrolysis in the V1 domain, the proton is translocated to the second hemi-channel in the a-subunit releasing H^+ to the lumen. Illustrated according to the model of Forgac, 2007.

1.1.2 Role and Relevance in Cancer Cells

It has been reported that cancer cells express V-ATPase on their plasma membrane to acidify the extracellular space, as low pH is important for invasion and proliferation (6–8). Expression of V-ATPase on the plasma membrane of breast cancer cells differs between highly metastatic and lowly metastatic cell lines. Cells with a more invasive phenotype had an increased V-ATPase expression and proton flux then non-invasive cell lines giving evidence that there is a correlation to the metastatic potential (8). It is known that cancer cells secret a variety of enzymes responsible for extracellular matrix degradation important for invasion and metastasis. These enzymes are most active at lower pH. Therefore, an acidification of the extracellular space is favorable for cancer cells (9). On the other hand plasma membrane V-ATPases may play an additional role in tumor cell growth and survival. Tumor cells are known to produce more H^+ due

to higher glycolytic activity (10). To circumvent cytosolic acidification the pH has to be tightly regulated. It has been shown that lactic acid accumulation due to enhanced glycolytic activity provokes the upregulation of several transporters including the V-ATPase resulting in a dysregulation of the solid tumor milieu favoring progression, invasion and metastasis (11).

1.1.3 V-ATPase Inhibitors

V-ATPases were shown to be overexpressed in highly metastatic cancer cells (8,12,13). There is also evidence that cancer cell treatment can enhance V-ATPase expression (14), on that account V-ATPase inhibitors might serve as potent anti-cancer drugs or sensitizer.

1.1.3.1 Bafilomycins and Concanamycins

Bafilomycins and concananmycins belong to the class of plecomacrolides first isolated from *Streptomyces* species already identified in the early 1980s (15–19). Bafilomycin was described as the first specific and highly potent V-ATPase inhibitor (18) but later concanamycin proved to have even higher specificity and inhibitory effects compared to bafilomycin (19,20).
For both inhibitors it has been shown that they bind to the c-subunit in the V0 domain (21–24), suggesting a rotation block of the proteolipid c-subunit ring relative to the a-subunit or additionally preventing conformational changes in c-subunit and thereby inhibiting V-ATPase activity (23,25).

1.1.3.2 Benzolactone Enamides

A variety of cytotoxic compounds sharing a benzolactone enamide core structure showed V-ATPase inhibitory potential comparable to plecomacrolides (26). All of them were first isolated from a variety of microorganisms such as marine sponges (salicylhalamides), tunicates (lobatamides), bacteria (oximidines) or myxobacteria (apicularen, cruentaren) (27).
Recently, the binding site for apicularen was investigated showing that apicularen binds the c-subunit in the V0 complex near the binding sites of plecomacrolides suggesting a similar mode of inhibition (28).

1.1.3.3 Indolyls

These are simplified synthetic structures based on bafilomycin with still active V-ATPase inhibitory function, developed after characterization of the key structural elements responsible for the biological activity of bafilomycin (29,30). They are widely used for V-ATPase research as they can be modified for different biophysical technics and approaches (31–33).

1.1.3.4 Archazolid a Macrolactone

Archazolid is a myxobacterial secondary metabolite, first isolated from *Archangium gephyra* and *Cystobacter violaceus* (34,35) binding c-subunit in the V0 domain of the V-ATPase and thereby inhibiting its activity (36). Archazolid was tested to be a highly specific V-ATPase inhibitor with no effect on F-ATPases or Na^+/K^+-ATPases and an IC_{50} in the nanomolar range (36). Archazolid binds in the equatorial region of the c-subunit rotor in the V0 domain within helix four of the c-subunit and not like bafilomycin at the interface between two adjacent c-subunits. Still the mode of action is assumed to be the same as for bafilomycin by blocking the rotation of the c-ring relative to the a-subunit or shielding the glutamate residue essential for proton binding to the c-subunit (37).

For archazolid A and B a total synthesis was achieved published 2007 and 2009 (38,39)

Archazolids are composed of a macrocyclic lactone ring with a thiazole side chain (Figure 3)(27).

In the last few years our group showed that archazolid is affecting motility of invasive cancer cells as well as induction of apoptotic cell death (40–42). We therefore hypothesized that archazolid might also affect the initial steps of metastatic dissemination which is characterized by the ability of invasive tumor cells to survive in a state of detachment from the extracellular matrix (ECM) (43).

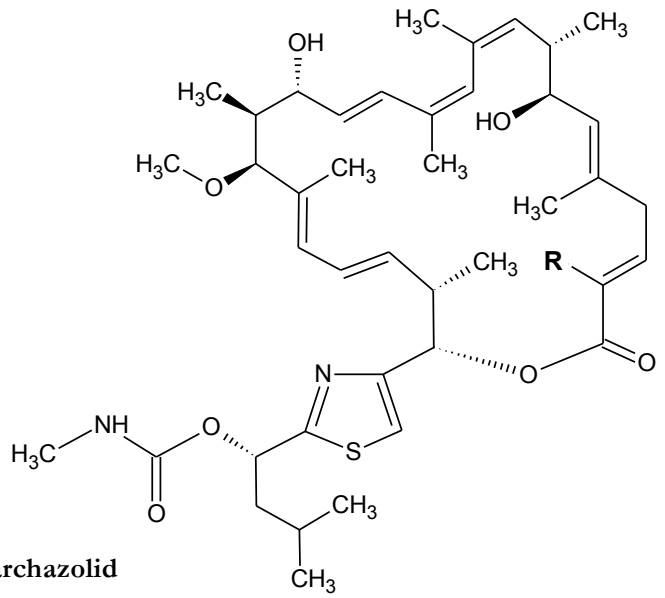

Figure 3: Structure of archazolid
R= CH_3: archazolid A
R= H: archazolid B
Structure adapted from Huss et al., 2009 (27)

1.2 Anoikis

Anoikis is a term first introduced by Frisch et al., 1994 describing the phenomenon that cells deprived of extracellular-matrix-attachment underwent classical apoptosis. They defined the expression anoikis for this occurrence, meaning "the state of being without a home, or homeless; Greek" (44). The significant findings of this paper were firstly, that attachment signals are mandatory to prevent activation of programmed cell death and that integrins play a crucial role in this event. Secondly, that detachment-induced-apoptosis requires the mitochondrial permeabilisation as known for the intrinsic apoptotic pathway and thirdly, that sensitivity towards anoikis differs significantly between cell types (45).

Anoikis is a specific type of apoptosis initiated by detachment of cells from their respective ECM. This is an important physiological process to maintain tissue homeostasis (46).

Anoikis is comprised of elements of the intrinsic and extrinsic apoptotic pathway together with the loss of survival signals. Vachon (2011) proposed a "four-punch" hypothesis for cell death induction by detachment. The first "punch" is the deactivation of integrin downstream signals like the focal adhesion kinase (FAK) and/or c-Src kinase and thereby inhibition of the PI3K/Akt and Ras/Raf/MEK/ERK survival pathway. As second "punch" he determined the simultaneous disassembly of anchoring focal adhesions largely by loss of integrin-mediated adhesion and destabilization of the cytoskeleton. The third "punch" is described as the activation of pro-apoptotic proteins triggering intrinsic apoptosis. The fourth "punch" finally is the induction of the extrinsic apoptotic pathway by caspase-8 activation (47).

1.2.1 Loss of Adhesion-Signaling

Anoikis is initiated by the disruption of integrin ligation to the ECM. Integrin binding activates distinct cell survival signaling cascades comprising downstream players such as FAK, c-Src kinase, PI3K/Akt and the extracellular signal-regulated kinase (ERK). Detachment of cells, meaning, loss of integrin signaling not only inhibits survival signals but also activates specific apoptotic processes (45,47,48).

The survival cascades activated via integrin ligation inhibit pro-apaptotic players like the Bcl-2 protein-family members BIM, Bad, Bax as well as several caspases and activate, transcriptionally or by direct interactions, anti-apoptotic players like the FLICE-like inhibitory protein (c-FLIP) (45,47,49). It has also been demonstrated that production of moderate levels of reactive oxygen species (ROS) upon integrin engagement can transduce pro-survival signals protecting from anoikis by activating kinases (Figure 4) (50).

Consequently, disruption of the integrin signaling inactivates kinase phosphorylation and pro-survival signal transduction and additionally triggers changes in the cytoskeleton releasing and activating pro-apoptotic proteins (47). Also ROS levels drop dramatically when cells are in suspension depriving them of the beneficial kinase activating function (50,51).

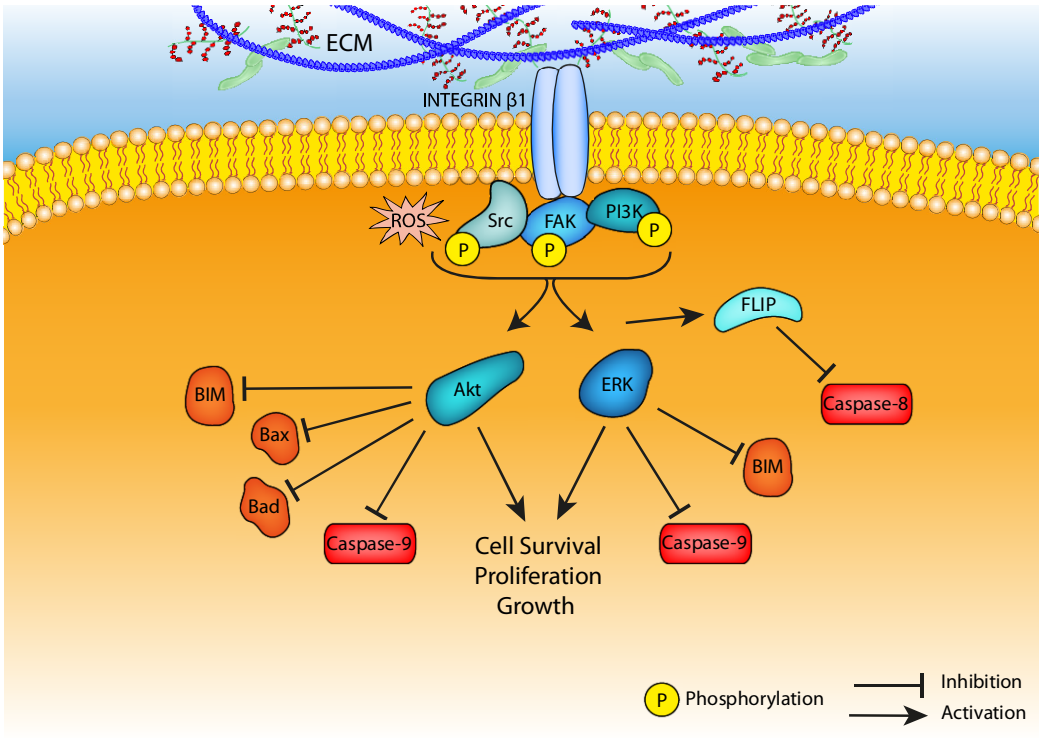

Figure 4: Integrin signaling upon ECM attachment
Integrin-ECM interaction recruits and activates several kinases like the focal adhesion kinase (FAK), PI3K and c-Src activating downstream Akt, ERK and c-FLIP, leading to the inhibition of pro-apoptotic proteins. On the other hand activated Akt and ERK initiate pro-survival and proliferative signaling cascades leading to cell growth.
Figure adapted from Charugi et al., 2008 and Vachon, 2011

1.2.2 Induction of the Intrinsic and Extrinsic Apoptotic Pathway

Anoikis, in line with classical apoptosis can follow the extrinsic pathway, triggered by cell surface death receptors or the intrinsic pathway driven by activation of pro-apoptotic proteins leading to permeabilization of mitochondria (46,52). Activation of caspase-8 is considered as a major player of the extrinsic pathway and the activation of pro-apoptotic members of the Bcl-2 family, in particular the protein BIM and mitochondrial cytochrome C release are features of the intrinsic pathway of anoikis. However, a crosstalk between intrinsic and extrinsic pathways frequently occurs (Figure 5) (53–55).

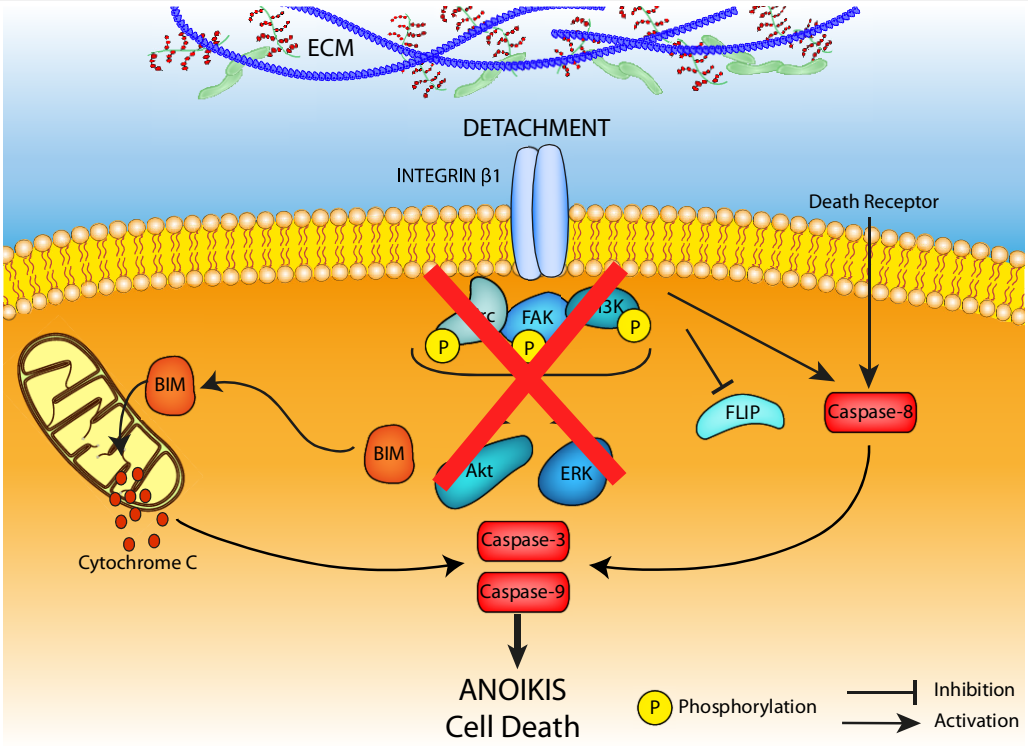

Figure 5: Detachment induced cell death – anoikis
Detachment induced cell death is initiated by the loss of integrin-ECM engagement leading to the loss of survival signals mediated by FAK, c-Src and the PI3K pathway. Disruption of focal adhesions also leads to cytoskeletal instability by loosing the direct ECM-cytoskeletal link. Next, pro-apoptotic proteins like BIM are activated, followed by cytochrome C release from the mitochondria. Together with active caspase-8 triggered by death receptors or unligated integrins effector caspases are cleaved conducting programmed cell death.

1.2.3 The Role of BIM in Anoikis Induction

BIM is thought to be a major inducer of the intrinsic anoikis pathway as it has been reported that BIM increases rapidly after detachment of anoikis sensitive cells. Additionally, downregulation of BIM by RNA interference (RNAi) inhibited anoikis in these cells. Detachment-induced expression of BIM requires integrin β1 detachment, downregulation of EGF receptor and inhibition of ERK signaling (48,54). BIM expression and release is tightly regulated. On the one hand BIM can be sequestered by the myosin motor complex when cells are ECM-attached (56). On the other hand the Akt pathway inhibits BIM gene-transcription and active Akt as well as active ERK phosphorylate BIM to be degraded by the proteasome or otherwise removed from the cytosol (57,58).

If BIM is released upon detachment it translocates to the mitochondria leading to cytochrome C release by activation of Bax and Bak oligomerization triggering classical apoptotic pathways like the apoptosome formation, caspase activation and DNA fragmentation (59,60).

Detachment triggers BIM release and increase in three ways. Firstly, it is set free from the myosin motor complex and accumulates in the cytosol, secondly Akt no longer inhibits BIM expression and thirdly attenuated Akt and ERK signaling inhibit proteasomal degradation and sequestration of the released BIM, which all together leads to increased BIM occurrence in the cytosol.

1.2.4 Caspase-8 Induction by Detachment

Caspase-8 activation as key feature of the extrinsic apoptosis-induction is reported to be involved in anoikis. Caspase-8 can induce apoptosis in two ways: High caspase-8 activation is sufficient to activate effector caspases leading directly to cell death, as low caspase-8 activation triggers the mitochondrial pathway via Bid cleavage. Cleaved Bid indirectly activates effector caspases via cytochrome C release. The mode of action of how caspase-8 induces cell death is also cell type specific (45,47,55). Caspase-8 is predominantly activated by death receptors binding death ligands (tumor necrosis factor-α, FasL, TRAIL) recruiting the Fas-associated death domain protein (FADD). FADD together with procaspase-8 form the death inducting signaling complex (DISC) resulting in cleavage and thereby activation of caspase-8 (47). Detachment induced apoptosis is clearly supported by the induction of caspase-8. There is evidence that caspase-8 can be recruited and activated by unligated integrins (61). Additionally, ligand bound integrin can indirectly inhibit procaspase-8 cleavage: FAK, c-Src and the MAP-kinase pathway hamper procaspase-8 from being activated, either by inhibiting the autoproteolytic activation of procaspase-8 or preventing FADD recruitment to form the DISC complex. This is implemented by phosphorylation of either the FADD or procaspase-8 or by activation of c-FLIP a known caspase-8 suppressor (46,47,62,63).

1.3 Anoikis Resistance and Metastasis

Whereas non-tumoral cells respond to loss of cell-matrix contact by induction of anoikis (44,64), metastatic cancer cells are resistant. This allows their survival after detachment from the primary tumor and their travel through the bloodstream to distant organs (44,64). In other words, anoikis resistance is a prerequisite and a hallmark for the metastatic spread of tumor cells (52). Integrin signaling has also been connected with chemoresistance as it can reduce drug- and even radiation-induced apoptosis (63).

Inducing anoikis by drugs is a promising option for the treatment of metastatic cancer but calls for a profound understanding of the mechanisms underlying anoikis resistance in invasive cancer.

Therefore, anoikis resistance mechanisms will be more deeply elucidated in the upcoming sections and are summarized in Figure 6.

1.3.1 Integrin Alterations

A strategy to evade anoikis is a switch in the integrin repertoire either by modifying integrin expression or changing the existing repertoire (56). As integrins are composed of two subunits (α and β) and each αβ combination has special binding and signaling properties (65) a switch from anoikis-sensitizing integrins to anoikis-suppressing ones is desired. This was described e.g. for squamous cell carcinoma as unligated αvβ5 triggered apoptosis whereas αvβ6 activated the PI3K/Akt pathway (66). Another example is unligated integrin β3, which can recruit and activate c-Src causing tumor cell survival. Therefore targeting cancer with specific integrin antagonists is a promising approach in tumor treatment and already tested in Phase II clinical trials (67). Integrins are also known to collaborate with growth factor receptors. Integrins can activate growth factor receptors in a ligand-independent manner by organizing signaling platforms (63). These signaling platforms are cholesterol-enriched membrane microdomains (CEMMs) regulating the localization and coupling of effector molecules and are normally internalized following detachment. This is mediated by caveolin-1 (Cav1) as Cav1 absence impairs CEMM internalization leading to increased signaling through e.g. Ras/Raf/MEK/ERK and PI3K/Akt (68).

1.3.2 Activation of Pro-Survival Signaling

To bypass signaling that would lead to anoikis, tumor cells can constitutively activate downstream pro-survival pathways (e.g. PI3K/Akt, ERK) by autocrine secretion of growth factors or over-expression of different receptor tyrosin kinases transducing survival signals (56).
To circumvent activation of the extrinsic apoptotic pathway malignant cells overexpress c-FLIP, an endogenous antagonist of caspase-8 with higher affinity for the DISC (52,55).

1.3.3 Targeting BIM Induction

By detachment BIM accumulates in the cytoplasm and translocates to the mitochondria triggering cytochrome C release leading to caspase-9 and caspase-3 activation inducing cell death. BIM is a key player in anoikis induction in various cancer cells. Therefore, metastasis requires attenuation of BIM. This can be achieved again by constitutive activation of Akt and ERK responsible for BIM degradation and transcription (69,70).

1.3.4 Reactive Oxygen Species

As mentioned, moderate levels of ROS induced by integrin engagement can activate c-Src kinases enhancing survival (50). Elevated ROS levels are often reported in solid tumors and cancer cell lines changing the tumor micro-enviroment (52). Oxidative stress in tumor cells is controversially discussed: On the one hand elevated ROS levels contribute to anoikis induction as the level of ROS was shown to correlate with the extend of cell death (71). On the other hand, elevated ROS levels are detected during metastasis with a protective effect as treatment with ROS scavenger increased apoptosis (50). If ROS production is beneficial for tumor cells it is probably context and level dependent.

1.3.5 Other Mechanisms

Anoikis resistance can be achieved through many different actions. One additional survival strategy is the induction of autophagy by detachment, a survival mechanism preventing anoikis. It has been shown that inhibition of autophagy increased caspase-3 activity in detached cells enhancing apoptosis (72). BIM was also suggested to play a role in autophagy by interacting with beclin-1 and inhibiting autophagosome formation (73). Autophagy can be used to survive unfavorable conditions like hypoxia or nutrition shortage by driving cells in a dormant state, with reactivation of metabolism and cell cycle when conditions improve, important for cancer cell metastasis. In anoikis resistance the reduced integrin signaling induces autophagy delaying the onset of apoptosis by sustaining ATP levels (56,74,75). It has been shown that specific blockage of β1 integrins is sufficient to induce autophagy. There are several ways described how ECM signaling can influence the autophagy machinery. One proposed mechanism is, that FAK, the downstream target of integrin, can indirectly inhibit mTOR. As mTOR is a classical autophagy inhibitor, loss of FAK leads to mTOR inhibition activating autophagy (74).

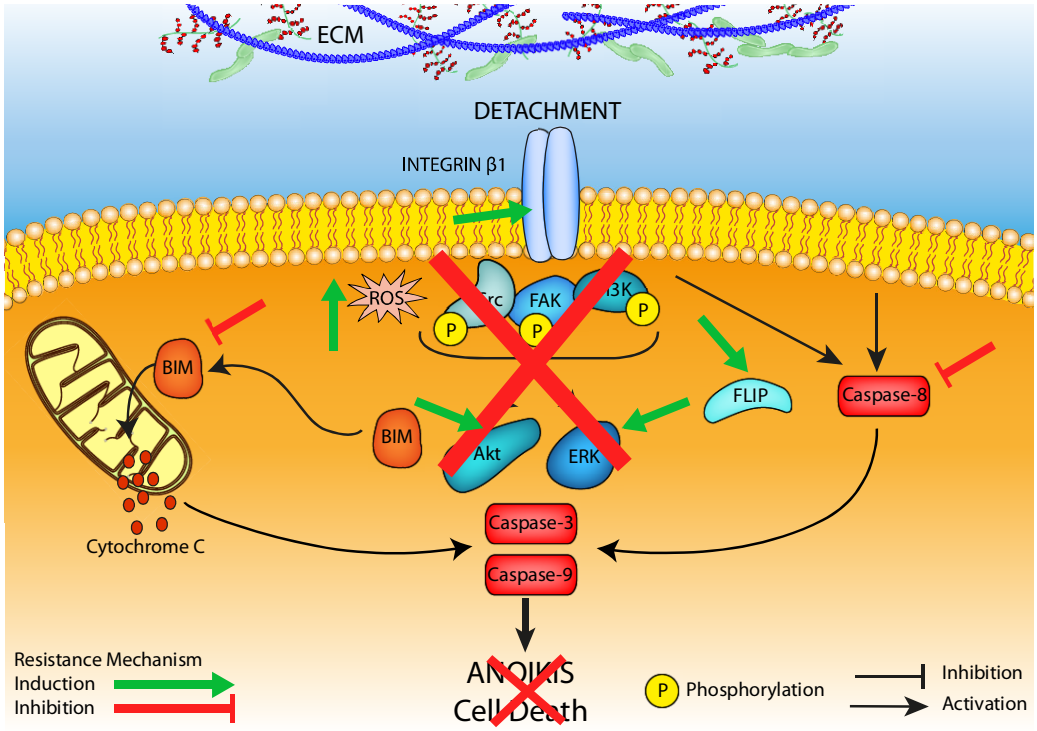

Figure 6: Anoikis resistance mechanisms

Anoikis resistance can be achieved by multiple actions. Cells can change or overexpress their integrin repertoire or activate survival kinases ligation independent. Inducing the proteasomal degradation of BIM or inhibiting BIM expression is another strategy to avoid cell death. By overexpression of c-FLIP, caspase-8 activation is repressed. Additionally, induction of ROS can activate survival kinases.

1.4 Aim of the Study

The cause of death by cancer is mainly not the primary tumor but the development of metastases in distinct organs (76). Metastasis is a highly complex process following sequential steps that comprise dissociation of cancer cells from the site of origin, their survival and travel in the circulation as well as migration and proliferation in distinct target organs (55,75,77). Due to the clinical importance there is still the need to better understand the major determinants of metastasis and to identify therapeutical targets and pathways suitable for fighting the metastatic process.

Our Group recently introduced the V-ATPase as a promising new anti-metastatic target showing that the V-ATPase inhibitor archazolid inhibits cancer cell migration (Figure 7) (40).

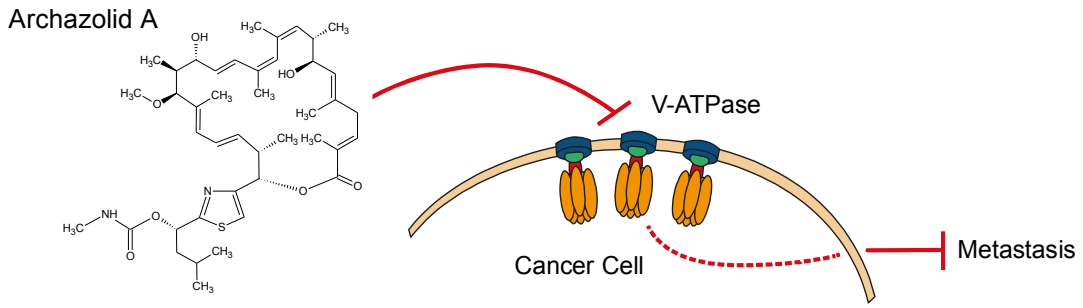

Figure 7: V-ATPase inhibition blocks metastasis
It was shown that V-ATPase inhibition by archazolid diminishes cancer cell migration and metastasis.

One prerequisite for cancer cell metastasis is the ability of cancer cells to detach from the solid tumor and survive and travel in the bloodstream to form metastasis. Normal tissue cells are prevented to detach and colonize elsewhere by a process called anoikis. This is a type of apoptotic cell death induced by the loss of cell-to-extracellular matrix connection.

The aim of this study was to investigate the effects of archazolid A on anoikis resistant tumor cells and to reveal if anoikis specific pathways are activated due to archazolid treatment.

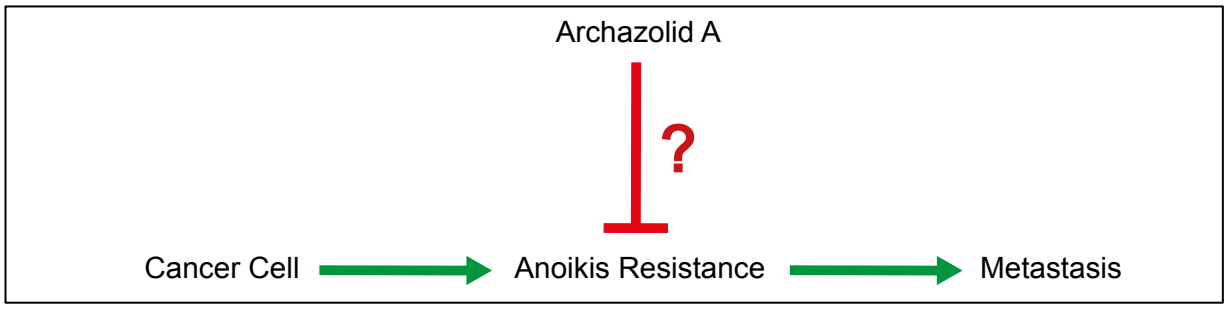

MATERIALS & METHODS

2 MATERIALS & METHODS

2.1 Materials

2.1.1 Compounds

Archazolid A was purified and isolated as described previously provided by the group of Rolf Müller (35). Concanamycin A was purchased from Enzo Life Science GmbH (Lörrach, Germany). Both compounds were solved in DMSO and stored at -20°C.

2.1.2 Chemicals, Inhibitors, Dyes and Reagents

Table 1: Inhibitors

Inhibitor	Distributor/Producer
Bortezomib (proteasome-inhibitor)	Selleck Chemicals, Munich, Germany
Complete® mini EDTA free	Roche diagnostics, Penzberg, Germany
LY 294002 (Akt-inhibitor)	Selleck Chemicals, Munich, Germany
MG-132 (proteasome-inhibitor)	Selleck Chemicals, Munich, Germany
Na_3VO_4	ICN Biomedicals, Aurora, OH, USA
NaF	Merck, Darmstadt, Germany
PD 98059 (ERK-inhibitor)	Selleck Chemicals, Munich, Germany
Phenylmethylsulfonyl fluoride (PMSF)	Sigma-Aldrich, Taufkirchen, Germany
Saracatinib (Src-inhibitor)	Selleck Chemicals, Munich, Germany

Table 2: Dyes, reagents and chemicals

Reagent	Distributor/Producer
Accustain® paraformaldehyde (PFA)	Sigma-Aldrich, Taufkirchen, Germany
Ac-LETD-AFC (caspase-8)	Bachem, Bubendorf, Germany
Agarose SeaPlaque® (low melting temp.)	Lonza Rockland, ME, USA
Bovine serum albumin (BSA)	Sigma-Aldrich, Taufkirchen, Germany
BCA Protein Assay Reagent (Kit)	Thermo Fisher Scientific, Schwerte, Germany
DCFDA (2',7'-dichlorofluorescin diacetate)	Sigma-Aldrich, Taufkirchen, Germany
DMEM (high glucose)	PAA Laboratories, Pasching, Austria
Dimethylsulfoxid (DMSO)	AppliChem, Darmstadt, Germany
EDTA	Carl Roth, Karlsruhe, Germany
EGTA	AppliChem, Darmstadt, Germany
Fetal calf serum gold (FCS gold)	PAA Laboratories, Pasching, Austria
Fibronectin	BD Bioscience, Heidelberg, Germany
FluorSave™ Reagent mounting medium	Merck, Darmstadt, Germany

Glutamine	Sigma-Aldrich, Taufkirchen, Germany
Glycine	Sigma-Aldrich, Taufkirchen, Germany
Hoechst (bisBenzimide H33342)	Sigma-Aldrich, Taufkirchen, Germany
LysoTracker® dye	Moleculare Probes, Darmstadt, Germany
McCoy´s Medium	PAA Laboratories, Pasching, Austria
Methylcellulose	Sigma-Aldrich, Taufkirchen, Germany
MTT (Thiazolyl Blue Tetrazolium Bromide)	Sigma-Aldrich, Taufkirchen, Germany
N-Acetyl-L-Cystein (NAC)	Sigma-Aldrich, Taufkirchen, Germany
Na-luciferin	Promega Cooperation, Madison, WI, USA
Non-fat dry milk poweder (Blotto)	Carl Roth, Karlsruhe, Germany
Page Ruler^{TM} Prestained Protein Ladder	Fermentas, St. Leon-Rot, Germany
Penicillin/Streptomycin 100x	PAA Laboratories, Pasching, Austria
Polyacrylamid (Rotiphorese® Gel A 30%)	Carl Roth, Karlsruhe, Germany
Poly(2-hydroxyethyl methacrylate) (Poly-HEMA)	Sigma-Aldrich, Taufkirchen, Germany
Propidium Iodide	Sigma-Aldrich, Taufkirchen, Germany
Rhodamin-Phalloidin (R415)	Invitrogen, Karlsruhe, Germany
RPMI 1640	PAN Biotech, Aidenbach, Germany
Triton X-100	Merck, Darmstadt, Germany
Trypsin	PAN Biotech, Aidenbach, Germany
Tween®100	BDH/Prolabo®, Ismaning, Germany

All other biochemicals, reagents and dyes not listed in Table 2 were purchased either from Sigma-Aldrich, AppliChem, Carl Roth or Merck.

2.1.3 Buffer and Media

Table 3: Commonly used buffers

Buffer	Composition
PBS (pH 7.4)	NaCl (123.2mM), Na_2HPO_4 (10.4mM), KH_2PO_4 (3.2mM) in H_2O
PBS+ Ca^{2+}/Mg^{2+} (pH 7.4)	NaCl (136.9mM), KCl (2.7mM), Na_2HPO_4 (8.1mM), KH_2PO_4 (1.5mM), $MgCl_2$ (0.5mM), $CaCl_2$ (0.7mM) in H_2O
DMEM	DMEM high glucose (500ml), FCS gold (50ml), Penicillin (10,000U/ml)/Streptomycin (10mg/ml) (5ml)
RPMI	RPMI 1640 (500ml), FCS gold (50ml), Penicillin (10,000U/ml)/Streptomycin (10mg/ml) (5ml)
McCoy´s	McCoy´s (500ml), FAC gold (50ml), Glutamine (1.5mM, 5ml), Penicillin (10,000U/ml)/Streptomycin (10mg/ml) (5ml)
Trypsin/EDTA	Trypsin (0.05%), EDTA (0.02%) in PBS
HFS-solution	Sodium citrate (0.1%), Triton X-100 (0.1%) in PBS

Table 4: Buffers for protein lysis and Western blot analysis

Buffer	Composition
Phospho-lysis buffer (pH 7.5)	EDTAx2H_2O (2mM), NaCl (137mM), Glycerol (10%), $Na_4P_2O_7$x10H_2O (2mM), Tris-Base (20mM), Triton X-100 (1%), $C_3H7Na_2O_6Px5H_2O$ (20mM), NaF (10mM), Na_3VO_4 (2mM)*, PMSF (1mM)*, Complete® mini EDTA free (4mM)*in H_2O
Digitonin lysis buffer** (pH 7.2) (mito-fractionation)	Mannitol (210mM), Sucrose (200mM), Hepes (pH 7.2, 10mM), Na_2EGTA (0.2mM), Succinate (5mM), BSA (0.15%), Digitonin (80µg/ml) in H_2O
5X SDS sample buffer	TrisHCl (pH 6.8) (3.125mM), Glycerol (10ml), SDS (5%), DTT (2%), PyroninY (0.025%), in H_2O
Stacking gel	Polyacrylamid solution (40%), Tris HCl pH 6.8 (125mM), SDS (0.1%), TEMED (0.2%), APS (0.1%) in H_2O
Separation gel 12%	Polyacrylamid solution (40%), Tris HCl pH 8.8 (375mM), SDS (0.1%), TEMED (0.1%), APS (0.05%) in H_2O
Elektrophoresis buffer	Tris-Base (4.9mM), Glycine (38mM), SDS (0.1%) in H_2O
Tank buffer 5X	Tris-Base (240mM), Glycine (195mM), in H_2O
Tank buffer 1X	Tank buffer 5X (20%), Methanol (20%) in H_2O
TBS-T (pH 8.0)	Tris-Base (24,76mM), NaCl (189.9mM), Tween 20 (0.1%) in H_2O

* added immediately before usage

** prepared ≤ 30min before usage

Table 5: Buffers for caspase activity measurement

Buffer	Composition
Lysis buffer	$MgCl_2$ (5mM), EGTA (1mM), Triton X-100 (0.1%), HEPES (25mM) in H_2O
Buffer B (pH 7.5)	HEPES (50mM), Sucrose (1%), CHAPS (0.1%) in H_2O
Substrate solution	Ac-LETD-AFC (56.25µM), DTT (0.2%) in Buffer B

2.1.4 Antibodies Used for Confocal Microscopy, Western Blot and FACS Analysis

Table 6: Primary antibodies used for immunoblotting

Antigen	Source	Dilution	In	Distributor/Producer
Actin	mouse	1:1,000	BSA 1%	Merck Millipore (MAB 1501)
Akt	rabbit	1:1,000	BSA 5%	Cell Signaling (9272)
Akt pSer473	mouse	1:1,000	Blotto 5%	Cell Signaling (4051)
BIM	rabbit	1:1,000	BSA 5%	Cell Signaling (2819)
COX IV	rabbit	1:1,000	Blotto 5%	Cell Signaling (4844)
Cytochrome C	rabbit	1:1,000	Blotto 5%	Cell Signaling (4272)
ERK	rabbit	1:1,000	Blotto 5%	Cell Signaling (9102)
ERK pThr202/Tyr204	mouse	1:1,000	Blotto 5%	Cell Signaling (9106)
FAK	mouse	1:1,000	BSA5 %	Santa Cruz (1688)
FAK pTyr397	rabbit	1:1,000	BSA 5%	Santa Cruz (11765)
c-FLIP	rabbit	1:1,000	BSA 5%	Cell Signaling (8510)
Src	mouse	1:1,000	Blotto 5%	Cell Signaling (2110)
Src pTyr416	rabbit	1:1,000	BSA 5%	Cell Signaling (6943)
Tubulin beta	rabbit	1:1,000	BSA 5%	Cell Signaling (2146)
VDAC	rabbit	1:1,000	BSA 5%	Cell Signaling (4866)

Table 7: Secondary antibodies used for immunoblotting

Antibody	Dilution	In	Distributor/Producer
Goat-anti-mouse IgG1 HRP	1:10,000	Blotto 1%	Biozol
Goat-anti-mouse IgG HRP	1:10,000	BSA 1%	Santa Cruz (2005)
Goat-anti-rabbit IgG HRP	1:10,000	Blotto 1%	Bio-Rad
Goat-anti-mouse IRDye® 800cw	1:20,000	Blotto 1%	Li-COR GmbH
Goat-anti-rabbit AlexaFluor® 680	1:20,000	Blotto 1%	Molecular Probes

Table 8: Primary and secondary antibodies used for confocal microscopy or FACS analysis

Antigen/Antibody	Dilution	Distributor/Producer
Integrin β1	1:400	Cell Signaling (4706)
Integrin β1 active form (12G10)	1:400	Abcam (30394)
Vinculin	1:100	Santa Cruz (25336)
Goat-anti-mouse AlexaFluor® 488	1:400	Molecular Probes
Goat-anti-rabbit AlexaFluor® 488	1:400	Molecular Probes

2.2 Methods

2.2.1 Cell Culture

The human urinary carcinoma cell line T24 was provided by Dr. B. Mayer (Surgical Clinic, LMU, Munich) in 2009 and authenticated in April 2013 by the DSMZ (Braunschweig, Germany) by DNA profiling of eight highly polymorph short tandem repeat (STRs) regions. Cells were cultured in McCoy´s medium supplemented as described in Table 3 at 37°C and 5% CO_2 (Heraeus, Hanau, Germany). MDA-MB-231 and 5637 cells were purchased from CLS cell lines service GmbH (Eppelheim, Germany) in May 2011 and April 2013. CLS authenticates all cell lines by DNA profiling via STR-analysis. The mouse breast cancer cell line 4T1-Luc2 was purchased from Caliper Life Science (USA) in January 2012. Caliper analyzed the cells by IMPACT 1 PCR profiling. 4T1-Luc2 and 5637 cells were maintained in RPMI-1640 medium and MDA-MB-231 cells in DMEM (High Glucose) (medium supplements see Table 3).

2.2.1.1 Passaging and Seeding

For passaging (1:10, every 3-4 days), growth medium was removed and cells were washed once with warm PBS. Cells were detached by incubation with 2ml Trypsin/EDTA for 5min at 37°C (75cm^2 flask). 7ml stopping-medium containing FCS was added to saturate the Trypsin. Cells were centrifuged (1,000rpm, 5min, RT), the pellet resuspended in medium and seeded in a new culture flask or well plate. To measure cell concentration and viability the VICELL™ cell viability analyzer (Beckman Coulter, Krefeld, Germany) was used.

2.2.1.2 Freezing and Thawing

For freezing, cells were harvested and counted as described in the previous section. Per cryovial 2x10^6 cells were pipetted, centrifuged (1,000rpm, 5min, RT), resuspended in 900µl freezing-medium containing 20% FCS and aliquoted in cryovials (900µl per vial). Now 100µl DMSO were added to each vial and stored at -20°C for 24h. Afterwards aliquots were moved to -80°C and finally stored in liquid nitrogen.

For thawing, the cryovial was warmed in a water bath to 37°C and the content was immediately dissolved in 10ml pre-warmed medium. To remove the remaining DMSO cells were centrifuged (1,000rpm, 5min, RT), resuspended in growth medium and transferred in a 25cm^2 cell culture flask.

2.2.2 LysoTracker Staining for Confocal Microscopy

To stain cells for confocal microscopy 70,000 cells/well were seeded on IBIDI slides (IBIDI, Martinsried, Germany) one day before treatment. After the indicated treatment time cells were stained with 250µl/well LysoTracker® dye (100nM) and Hoechst (0.05µg/ml, nuclei staining) in PBS+ for 30min, 37°C. Subsequently, cells were imaged by confocal microscopy (LSM 510 Meta, Zeiss, Oberkochen, Germany) without fixation.

2.2.3 Cell Adhesion by Impedance Measurements

The XCELLigence™ Real-Time Cell Analyzer (RTCA) system (Roche Diagnostics, Mannheim, Germany) was used to analyze adherence time of pretreated T24 cells. Therefore $5x10^3$ cells/well were seeded in the respective electrode plate (E-Plate 16) after 24h prestimulation. Cell impedance was measured and adhesion time analyzed using the manufacturer's software (Software RTCA 1.2.1). There, the impedance is expressed as Cell Index (CI) a dimensionless parameter based on relative impedance changes. The CI baseline is defined by the electric conductance of the medium and increases upon cell-electrode contact while cells adhere to the surface. The slopes over the first 4h were analyzed and compared.

2.2.4 Focal Adhesion Staining for Confocal Microscopy

T24 cells were seeded in 12-well plates (100,000 cells/well) and treated with archazolid (10nM, 24h) the day after. To stimulate focal adhesion formation, IBIDI slides (IBIDI, Martinsried, Germany) were coated with fibronectin (25µg/ml, 2h, 37°C then 2% BSA in PBS+, 1h, 37°C) before adding the cells (40,000 cells/well in 250µl growth medium). After 30min at 37°C incubation time cells were washed once with PBS+, fixed with 4% PFA (15min, RT) washed again and permeabilized with 0.1% Triton X-100 in PBS (2min, RT). Washed cells were blocked for 15min with 2%BSA/PBS+ to block unspecific binding. Thereafter, cells were incubated for 1h at 4°C with vinculin antibody diluted in 2%BSA/PBS. After three washing steps the secondary AlexaFluor® 488 antibody was applied together with rhodamine-phalloidine for F-actin staining (1h, dark, RT in 2%BSA/PBS). Again, cells were washed three times with PBS+ and embedded in FluorSave™ Reagent mounting medium and covered with a glass coverslip. Images were taken by confocal microscopy (LSM 510 Meta, Zeiss, Oberkochen, Germany).

2.2.5 In Vivo Experiments

Twenty, 4-6 weeks old female BALB/cByJRj mice (Janvier) were housed in individually ventilated cages with a 12h day/night cycle and food and water *ad libitum*. Mice were injected with archazolid pretreated (10nM, 24h) or untreated 4T1-Luc2 cells ($1x10^5$) via the tail vein. Bioluminescence of metastasized cells was monitored at day 8 after cell injection under anesthesia (2% isoflurane in oxygen) using the IVIS Lumina system with Living Image software 3.2 (Caliper Life Sciences) 15 minutes after intraperitoneal injection of 6mg Na-luciferin (Promega). Thereafter mice were sacrificed by cervical dislocation, their lungs harvested, imaged and weighted. The total flux/area of the defined region of interest was calculated as photon/second/cm^2. All *in vivo* experiments were performed according to the guidelines of the German law for protection of animal life and approved by the local ethics committee.
In vivo experiments were performed by Laura Schreiner and Rebekka Kubisch.

2.2.6 Colony Formation Assay

Archazolid treated T24 cells ($5x10^3$, 24h) were suspended in a 0.4% agarose-medium mix (50%/50%), (low melting temperature agarose, LONZA) and seeded on 6-well-plates precoated with 1% agarose. Cells were incubated for 9 days at 37°C to proliferate and form viable 3D colonies. Evolved colonies were stained with MTT dye, photographed and analyzed by ImageJ 1.46r software. On that account an ImageJ-macro was developed to automatize colony-counting and -size analysis.

2.2.6.1 ImageJ Macro

First, a circle with constant properties (h=966px, w=956px) was cut out of each photographed well, only containing stained colonies and no plastic surrounding and pasted in a new file. Pictures have to be in grayscale to be processed by this macro, otherwise they should be converted first.
Then the following macro was used on the file converting the photograph in a black and white picture were only stained colonies of a size between 2-20px appear black. The "Watershed" command was used to split overlaid colonies. At the end the macro releases a table with the number and size of all counted colonies.
To first adjust and then verify the accuracy of the macro three wells were counted by hand and compared to the results of the macro.

Table 9: ImageJ macro counting stained colonies from the colony formation assay

Macro commands (in sequence)	Meaning
run("Subtract Background...", "rolling=50 light");	Removes smooth, continuous, bright backgrounds behind dark objects based on the "rolling ball" algorithm
run("Sharpen");	Sharpens all objects in the image

setAutoThreshold("Default");
//run("Threshold...");
setThreshold(0, 197);
run("Convert to Mask");
	All colonies with an intensity over 197 are selected and converted to a binary black and white image, where selected colonies appear black

run("Watershed");	If some colonies are merged together they can be separated by this command
run("Analyze Particles...", "size=2-20 circularity=0.00-1.00 show=Masks display clear summarize record");	Now the size and number of the particles are analyzed and recorded in a table

2.2.7 Detachment-Induced Anoikis Assay

T24, MDA-MB-231, 4T1 or 5637 cells ($7x10^4$/well) were kept in suspension by using poly-HEMA (poly(2-hydroxyethyl methacrylate)) coated 24-well plates to prevent adhesion (78,79). Poly-HEMA was dissolved as a stock solution in 99% EtOH (120mg/ml). To coat culture dishes with poly-HEMA the stock solution was diluted right before use 1:10 with 99% EtOH and warmed in a water bath to prevent precipitation. All wells were filled with the solution until the bottom was completely covered and dried open under the flow for at least 3h until all EtOH evaporated. The growth medium was supplemented with 1% methylcellulose to increase viscosity to prevent cell clumping of the floating cells. Here, cells were treated with archazolid right after seeding them in poly-HEMA coated wells. Apoptotic death was analyzed as described by Nicoletti et al. (80). After the indicated treatment time, cells were harvested, transferred to FACS tubes, washed once with ice-cold PBS (600g, 5min, 4°C) and resuspended in HFS- or PBS-solution containing propidiumiodide. Permeabilized cells stained with propidiumiodide (PI, 50 µg/µl) were analyzed for their sub-diploid DNA content by flow cytometry (FACSCanto II, BD), as DNA fragmentation is characteristic for late apoptosis. Cell death was further analyzed by the PI exclusion assay counting PI positive (5µg/µl), non-permeabilized cells by flow cytometry. All experiments were analyzed by FlowJo 7.6 software.

2.2.8 Flow Cytometry Analysis of Cell Surface Integrin

Active integrin β1 on the cell surface was examined using a conformation specific integrin β1 antibody as for total integrin β1 a not conformation specific one was used. Floating and adherent cells were treated with archazolid (10nM, 24h), harvested on ice (adherent cells were trypsinized with trypsin/EDTA first), transferred to FACS tubes, washed once with ice-cold PBS (600g, 5min, 4°C) and incubated with the respective integrin β1 antibody (45min, 4°C in 0.01% BSA/PBS). After washing with PBS cells were incubated with a fluorescent secondary antibody (45min, 4°C in 0.01% BSA/PBS) and analyzed by flow cytometry. The experiments were analyzed by FlowJo 7.6 software.

2.2.9 Caspase Activity

After treating cells with archazolid (1nM, 10nM, 48h) the activity of caspase-8 was measured using a commercial caspase-8 activity assay (Calbiochem) based on the cleavage of a caspase-8 specific AFC (7-amino-4-trifluoromethyl coumarin) labeled peptide sequence. Therefore, cells were harvested, washed once with ice-cold PBS and lysed by the caspase lysis buffer and stored over night at -80°C. The next day, the cell lysat was centrifuged (14,000rpm, 10min, 4°C) to sediment cell debris and the supernatant was transferred to a new vial. Protein concentration was determined by the BCA assay.

For measurement 10µl of each sample was pipetted in a non-transparent 96-well plate in triplicates. Now, 90µl of the freshly made substrate solution containing the labeled peptide sequence was added to each well. The fluorometric shift over 5h at 37°C was monitored by a fluorescent plate reader (SpectraFluorPlus, Tecan, Männedorf, Austria) calculating the relative enzyme activity displayed as the relative fluorescence signal (RFU).

2.2.10 Intracellular ROS Level

Reactive oxygen species (ROS) were measured by using the 2′, 7′-dichlorofluorescin diacetate dye (DCFDA, Sigma-Aldrich), which is a cell-permeable non-fluorescent probe, trapped intracellular by de-esterification and fluoresces upon oxidation. Cells were harvested after incubation with the indicated substances and stained with 20µM DCFDA for 30min at 37°C, washed once with PBS and measured by flow cytometry (excitation 488nm, emission, exitation 535nm, FACSCanto II, BD). To exclude dead cells from the ROS measurement cells were double stained with DCFDA and PI. Accordingly, cells were stained for 30min with 5µg/ml PI in PBS at 4°C after the

DCFDA staining. The ROS scavenger N-Acetyl-L-Cystein (NAC) used in this study was previously dissolved in PBS (pH 7.4) before application.

2.2.11 Western Blot Analysis and Cytosol-Mitochondria Fractionation

Protein levels were investigated by Western blot analysis. Floating cells were treated with archazolid and the listed inhibitors for the indicated timeframes and subsequently lysed with phosphor-lysis buffer. Protein concentration was quantified by the bicinchoninic acid (BCA) protein assay according to the manufactures instructions. Equal amounts of the proteins were separated by SDS-PAGE (100V, 20min then 200V, 42min)(Bio-Rad System, Munich, Germany) and transferred onto nitrocellulose membranes by tank blotting (90V for 90min, 4°C). For detection of specific proteins, the ECL detection system (Amersham Pharmacia Biotech) or the Odyssey Infrared Imaging system version 2.1 (LI-COR Biosiences) was used.

For cytosol-mitochondria fractionation cells were harvested, incubated with the digitonin-lysis-buffer (20min, on ice) and centrifuged (10min, 1,300rpm, 4°C). The supernatant was collected (cytosolic fraction) and the pellet permeabilized with 0.1% TritonX-100 (15min, on ice) (mitochondrial fraction). Both fractions were centrifuged one more time (14,000rpm, 10min, 4°C) to sediment the cell debris. Mitochondrial and cytosolic fractions were then processed like normal Western blot lysates.

2.2.12 Statistics

All experiments were performed at least three times in triplicates. All statistic analysis were performed using GraphPad Prism 5.0 software.

One-way ANOVA with Turkey post-test and for two column comparison the unpaired Students t-test was performed as significance analysis. Error bars indicate standard errors of the mean (SEM).

RESULTS

3 RESULTS

3.1 Effects of Archazolid on Anoikis Resistant Cancer Cells

Anoikis resistant cancer cells are known to have highly invasive phenotypes (81). To overcome detachment induced cell death these cells have to activate several survival mechanisms probably influencing their response to chemotherapeutical treatment and enhancing their metastatic potential. Survival signals by adhesion are one of the major signaling cascades preventing anoikis (49).

Therefore, adherent and detached cancer cells were investigated and compared concerning their anoikis resistance and responses to archazolid treatment.

First, archazolid-functionality in inhibiting the V-ATPase was investigated in three different cell lines by surveying if acidification of intracellular compartments was blocked after archazolid treatment.

Second, the influence of archazolid on adhesion time and manifestation, carried out by impedance measurements and confocal staining of adhesion-structures, was observed.

Third, the impact of archazolid on anchorage independent growth as well as cell death induction was analyzed.

3.1.1 Alkalization of Lysosomes by Archazolid Treatment

To confirm that archazolid in fact inhibits the V-ATPase activity in our model cells, endolysosomal pH was monitored by staining cells with LysoTracker® dye (Figure 9). The dye is highly selective for acidic organelles where the fluorophore accumulates staining acid organelles red.

Archazolid is a specific V-ATPase inhibitor functional in the nano-molar range (36).

The V-ATPase is mostly located in the membrane of acidic organelles like the lysosomes or endolysosomes responsible for their acidification.

Adherent T24 (urinary), MDA-MB-231 (mammary) and 4T1 (mouse mammary) cancer cells were treated with different archazolid concentrations (5 and 10nM) for 2h (T24 cells) and 4h (MDA-MB-231 and 4T1). Thereafter cells were stained with LysoTracker® dye to monitor lysosomal pH in living cells using confocal microscopy.

Figure 9 confirms that acidification of cell organelles is blocked by 5 and 10nM archazolid after 2-4h of treatment in all investigated cell lines.

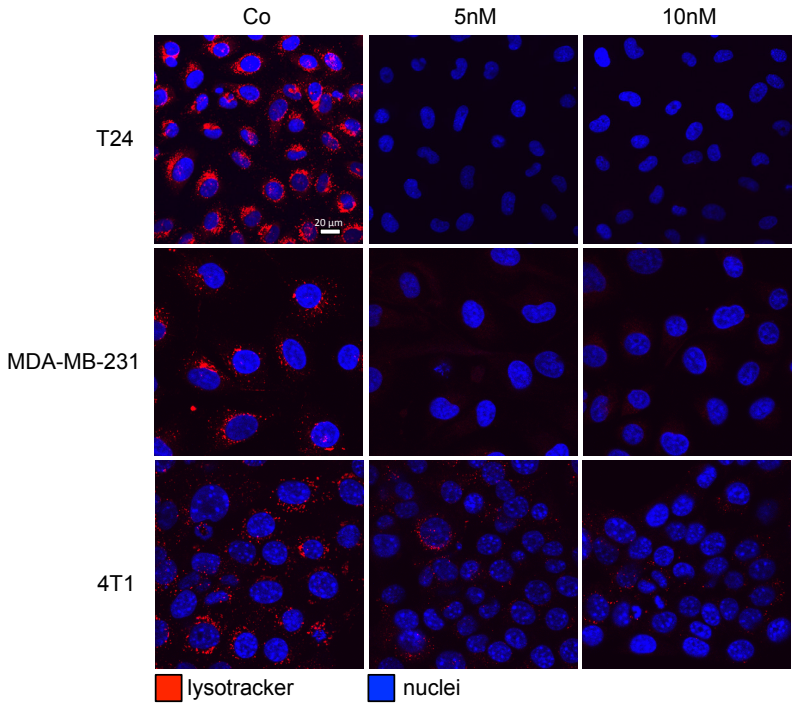

Figure 9: Alkalyzation of lysosomes by archazolid treatment

T24, MDA-MB-231 and 4T1 cells were treated with different archazolid concentrations (5 and 10nM) for 2h (T24 cells) and 4h (MDA-MB-231 and 4T1). Thereafter cells were stained for 30min at 37°C with LysoTracker® dye to monitor lysosomal pH using confocal microscopy.

3.1.2 Adhesion Ability is Impaired after Archazolid Treatment

To prove that archazolid treatment has an impact on adhesion and therefore on the adhesion signaling cascade, an adhesion assay was performed (Figure 10).

Adhesion molecules play a central role in anoikis induction and resistance. Anoikis resistant cells e.g. can change their integrin repertoire on the cell surface to circumvent integrin mediated death (IMD) or constitutively activate pro-survival downstream signals (56).

Adherent T24 cells pretreated with archazolid (10nM, 24h) were harvested and subsequently seeded out for impedance measurements in the XCELLigence system. For this, cells were suspended in 200µl medium in E-plate-wells and adhesion time between treated an untreated cells was monitored as an increase in impedance, indicated as Cell Index occurring while cells adhere to the surface.

The slopes of three independent experiments were calculated and the relative cell adhesion (%) was analyzed (Figure 10B). Figure 10 shows that adhesion time is prolonged after archazolid treatment, which suggests an effect of archazolid on cell adhesion.

If adhesion is altered by archazolid treatment one could assume that there is also an impact on the pro-survival signaling cascade.

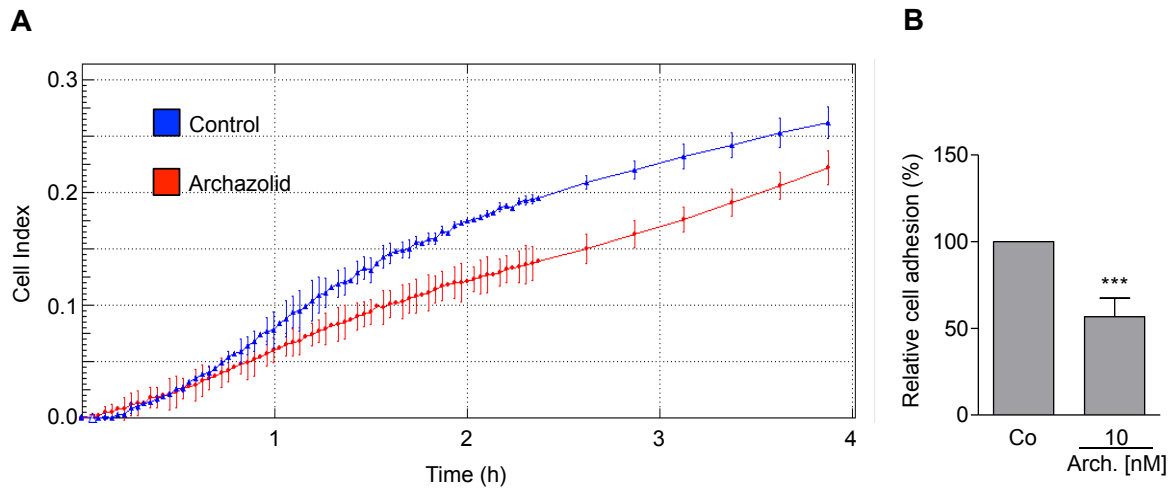

Figure 10: Prolonged adhesion time after archazolid treatment.
Adherent T24 cells were pretreated with archazolid (10nM, 24h) or left untreated.
The kinetics of cell adhesion was subsequently measured using impedance measurement in the XCELLigence system over 4h.
A: One representative graph out of three independent experiments is shown.
B: The slopes (Cell Index/Time) of three independent experiments conducted in triplicates were calculated and the relative cell adhesion (%) was analyzed were control cells are represented as 100% adhesion. Archazolid treated cells show a reduced adhesion compared to control cells.

3.1.3 Changes in Focal Adhesion

Adherent, archazolid treated cells were further analyzed by confocal microscopy to investigate changes in the focal adhesions. Therefore, cells were pretreated with archazolid (10nM, 24h) and subsequently seeded on fibronectin coated slides for 30min at 37°C. During the adhesion process cells develop focal adhesions, which can be stained by an antibody recognizing vinculin, a central protein in the focal adhesion plaques, and F-actin by rhodamine-phalloidin. Both proteins co-localize in focal adhesion shown by the merged picture (Figure 11).

Archazolid treatment clearly influences focal adhesion formation. Compared to control cells there is less vinculin clustering on the cell periphery. After treatment a more regular distribution of mature focal adhesions was observed.

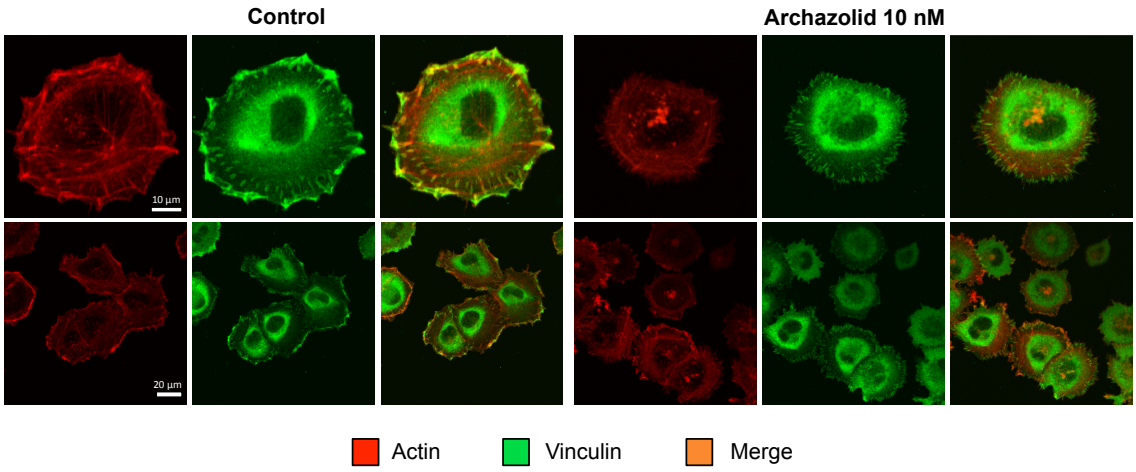

Figure 11: Changes in focal adhesions by archazolid treatment

T24 cells were prestimulated with archazolid (10nM, 24h) or left untreated, then harvested, suspended and seeded on fibronectin coated slides for 30min, at 37°C. After 30 min cells will form first focal adhesions with the surface. Cells were then fixed, permeabilized and stained for confocal microscopy. Control cells show more vinculin clustering on the cell periphery then archazolid treated cells.

The experiment was conducted three times in triplicates.

3.1.4 Archazolid Impairs Anchorage Independent Growth and Induces Anoikis in Invasive Cancer Cells

To show anoikis resistance of the invasive cancer cell lines T24, 5637 (urinary), MDA-MB-231 and 4T1 cells were grown in an anchorage-independent environment (Figure 12 and Figure 13) and subsequently analyzed for cell viability and cell death.

3.1.4.1 Colony Formation Assay

T24 cells were embedded in a soft agar layer without contact to ECM components or other cells to mimic anchorage independent growth. Untreated cells formed viable colonies after nine days of cultivation (Figure 12A, left, below) indicating anoikis resistance.

Pretreatment of adherent T24 cells with archazolid (1nM, 10nM, 24h) impaired anchorage-independent growth as shown by a reduction of viable colonies in the soft agar colony formation assay (Figure 12A left). Inhibition of colony formation in T24 cells could also be observed by the V-ATPase inhibitor concanamycin (Figure 12A right) suggesting a V-ATPase dependent effect.

To exclude apoptosis to be responsible for the obtained results, adherent, 24h treated cells were analyzed for cell death induction. Permeabilized cells were stained with PI to measure the sub-G1 DNA content as DNA fragmentation occurs during the apoptotic process (Figure 12B).

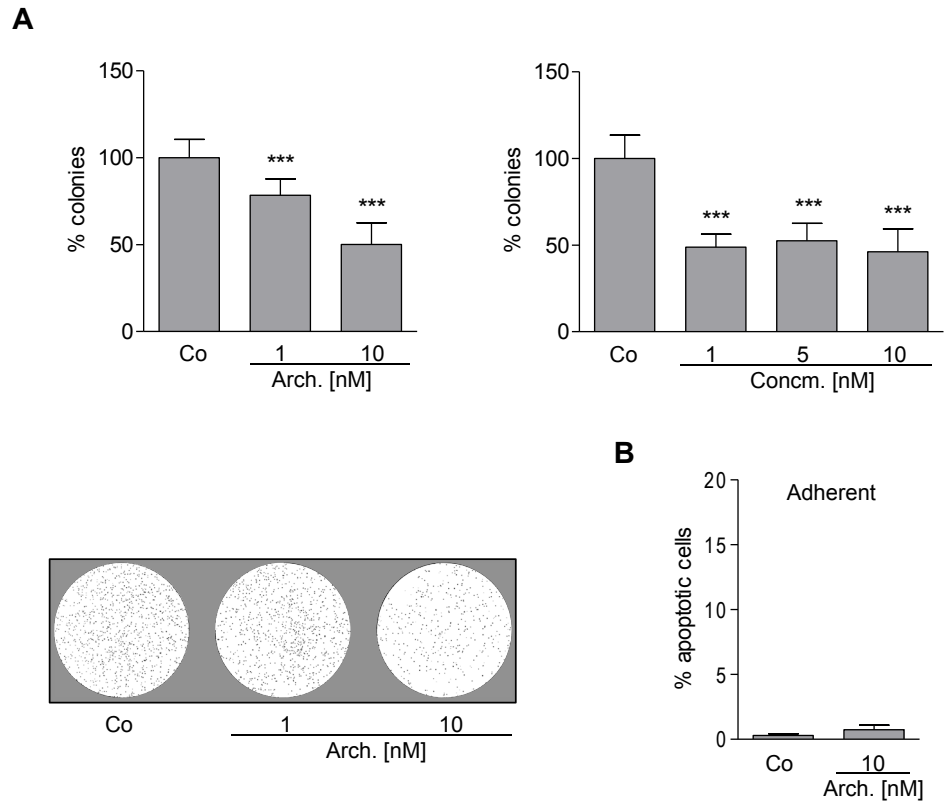

Figure 12: Anchorage independent growth is reduced by archazolid pre-treatment.

A: T24 cells were pretreated with archazolid (1 and 10nM, 24h), concanamycin (1, 5, and 10nM, 24h) or left untreated (Co) and subsequently cultured in a soft agar layer for nine days. Anchorage independent growth was analyzed by counting stained colonies (MTT). Bars represent the percentage of colony formation compared to control cells. ***P< 0.001, n=3. Lower left: Representative colonies of archazolid treated and untreated T24 cells are shown.

B: Adherent T24 cells were treated with archazolid for 24h (10nM). Apoptotic cell death was investigated as described in materials and methods. Bars represent the percentage of apoptotic cells as mean ± SEM of three independent experiments conducted in triplicates.

3.1.4.2 Analyzing Cell Death Induction in Detached Cells

To further analyze effects of archazolid on anoikis, cells were kept in a detached status using poly-HEMA coated culture dishes and medium supplemented with methylcellulose to prevent massive cell aggregation. This setup was used for all further experiments with floating cells.
Treatment with archazolid (10nM) induced anoikis in detached cancer cell lines T24, 5637 and 4T1 after 48h and MDA-MB-231 after 72h, respectively (Figure 13).

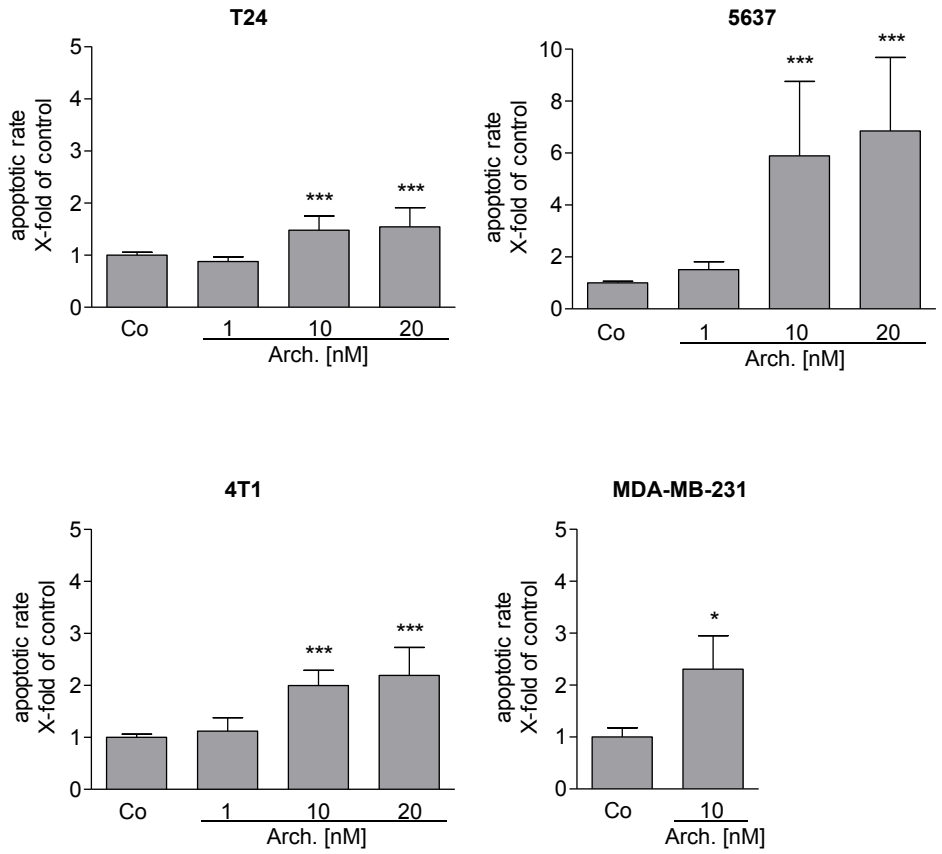

Figure 13: Induction of anoikis in detached cells by archazolid
Detached T24, 5637 and 4T1 cells were treated with different concentrations of archazolid for 48h and analyzed for apoptotic cell death. ***P<0.001, n=3. Detached MDA-MB-231 cells were treated with archazolid (10nM) for 72h and apoptotic cells were quantified by flow cytometry as described in materials and methods. *P<0.05, n=3. Bars represent the relative induction of apoptosis compared to control cells. Bars always represent the mean ± SEM of three independent experiments done in triplicates.

3.1.5 Cell Death Induction in Adherent and Floating Cells by Archazolid

To investigate the impact of detachment on cell death induction by archazolid adherent and floating cells were treated with archazolid (10nM, 24h or 48h) or left untreated.

As detachment and thereby loss of survival signals also affects anoikis resistant cells, the basal cell death level was expected to be elevated in floating cells (Figure 14). Noteworthy, archazolid did neither induce apoptosis in adherent nor floating cells after 24h of treatment compared to the respective control cells.

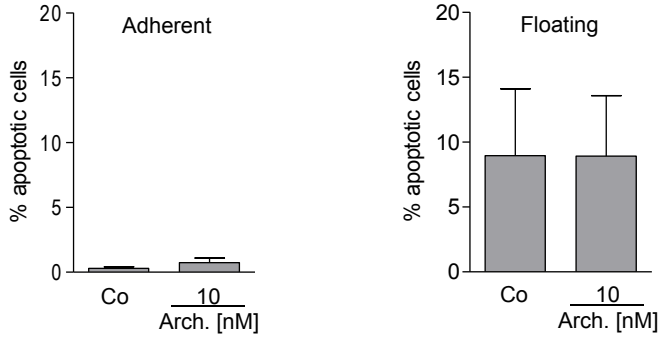

Figure 14: Influence of detachment on basal cell death level
Adherent and floating T24 cells were treated with archazolid for 24h (10nM). Apoptotic cell death was investigated as described in materials and methods. Bars represent the percentage of apoptotic cells as mean ± SEM of three independent experiments conducted in triplicates.

Cell death by archazolid did not occur before 48h of treatment.

To compare the cell death induction of adherent and floating cells independently of the basal cell death level, specific apoptosis was calculated as $\frac{treatment-control}{100-control} * 100$.

Calculating specific apoptosis, adherent T24 cells show a higher sensitivity towards archazolid after 48h then floating cells (Figure 15) pointing to death resistance or chemoresistance mechanisms induced by detachment.

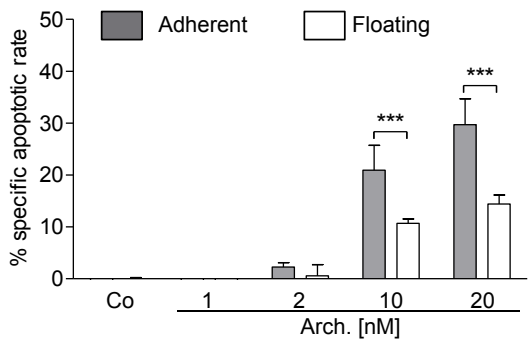

Figure 15: Adherent T24 cells are more sensitive to archazolid then floating cells
Adherent and floating T24 cells were treated with archazolid for 48h (1, 2, 10 and 20nM). Apoptotic cell death was investigated as described in materials and methods. Bars represent the specific apoptotic rate compared to control as mean ± SEM of three independent experiments done in triplicates. ***P<0.05.

3.2 Archazolid treated tumor cells lose their metastatic potential *in vivo*

The anoikis inducing effect of archazolid was hypothesized to affect the invasive potential of tumor cells *in vivo*. To confirm this hypothesis an *in vivo* model based on the 4T1-Luc2 mouse mammary tumor cell line has been used. These cells are highly metastatic and disseminate quickly to the lungs when injected intravenously and are therefore resistant to anoikis as anoikis resistance is a precondition for metastasis. 4T1-Luc2 cells are further engineered to express a luciferase reporter to enable real time monitoring of developing tumors by live imaging.

As shown in Figure 16 4T1-Luc2-injected animals formed easily detectable lung metastases, however 4T1-Luc2 cells pretreated with archazolid (10nM, 24h) showed a significant reduction of lung metastases (Figure 16B, left). Archazolid treated cells did not show signs of apoptosis at the time of the intravenous injection (Figure 16B, right).

In vivo experiments were performed by Laura Schreiner and Rebekka Kubisch.

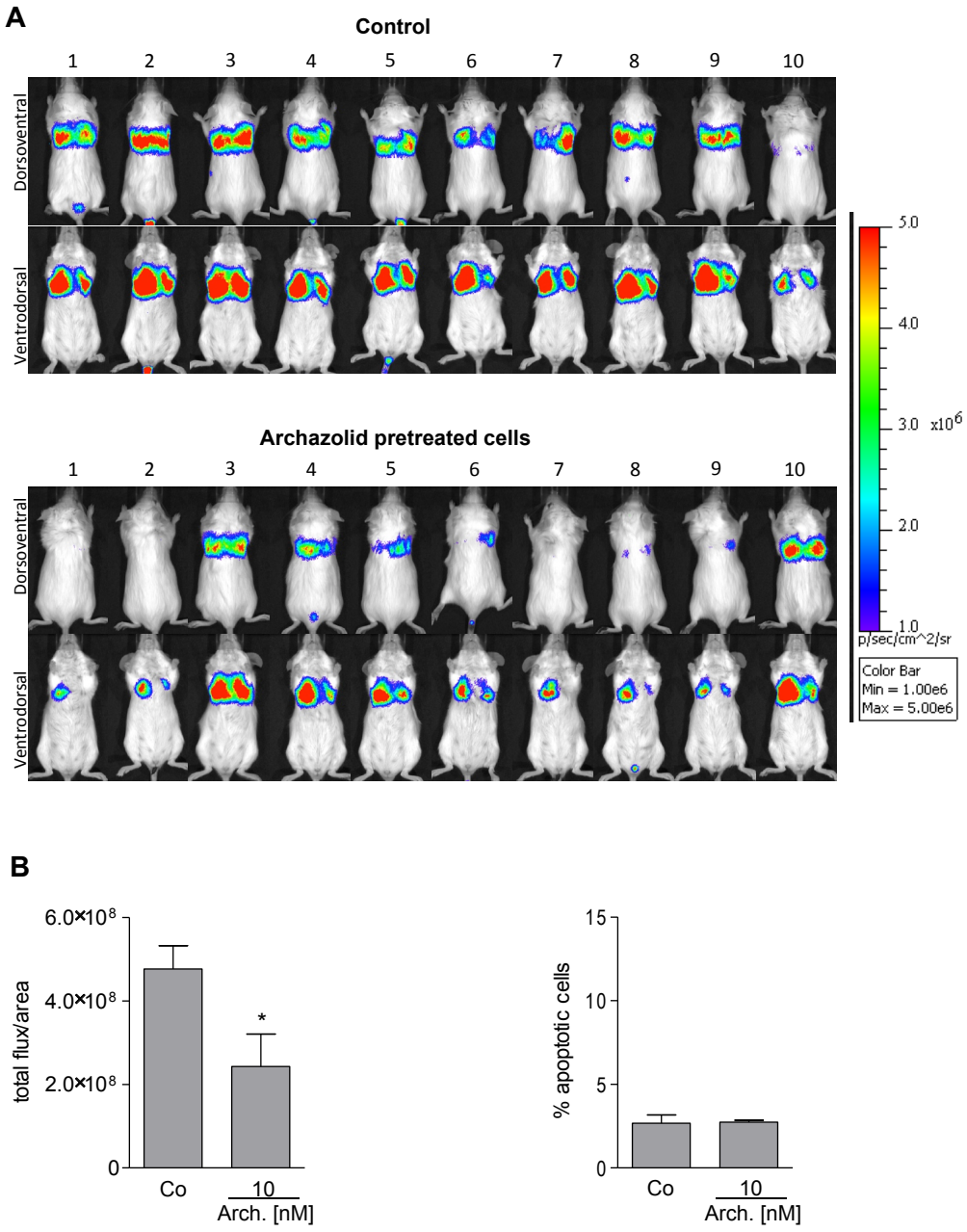

Figure 16: Pretreatment of invasive breast cancer cells with archazolid reduced metastasis in mice lungs

4T1-Luc2 cells were pretreated with archazolid (10nM, 24h) or left untreated and subsequently injected ($1x10^5$) in the tail vain of 10 BALB/cByJRj mice per group.

A: At day eight after inoculation lung metastases were monitored by bioluminescence read out by dorsoventral and ventrodorsal mice imaging.

B: Bioluminescence signals were calculated as total flux/area. Pretreated adherent cells were tested for apoptotic cell death three times in triplicates. Bars represent the mean ± SEM. *P<0.05, n=10

Performed by Laura Schreiner and Rebekka Kubisch.

3.3 Underlying Mechanisms of Anoikis Induction by Archazolid

3.3.1 Archazolid Treatment Reduces Active ß1 Integrin on the Cell Surface of Detached Cells

Integrin β1 is a major player responsible for cell adhesion to the ECM. Activated by attachment integrin β1 signaling inhibits anoikis and promotes cell survival (82).

In Figure 10 it has been shown that treatment with archazolid impairs adhesion abilities of T24 cells after 24h of treatment, suggesting an effect of archazolid on adhesion molecules such as integrins.

Figure 17A shows that the level of active integrin β1 (analyzed by an integrin β1 conformation specific antibody) is similar between adherent and detached (24h) T24 cells. However, archazolid treated (10nM, 24h), detached cells display a reduction of active integrin β1 compared to detached control cells, whereas surface level of total integrin β1 was not affected by archazolid treatment (Figure 17B).

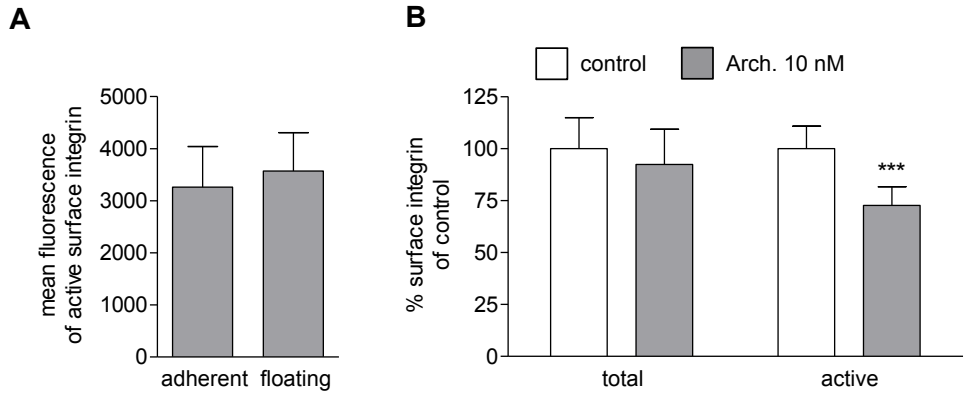

Figure 17: Archazolid treatment decreases active integrin β1 on the cell surface

A: Cell surface level of integrin β1 was analyzed by an antibody recognizing only active integrin β1 and compared between adherent and detached (24h) T24 cells. No differences in surface level of active integrin β1 between adherent and floating cells could be detected.

B: Levels of total and active integrin β1 on the cell surface of archazolid treated (24h), floating T24 cells was investigated by antibody staining and flow cytometry. Active integrin β1 is reduced on the cell surface of archazolid treated cells ***P<0.001, n=3

3.3.2 FAK Activity is Decreased in Detached Archazolid Treated Cells

The focal adhesion kinase is recruited and activated by integrins binding to their ECM ligands, leading to the activation of several downstream survival signals via the PI3K/Akt and the Raf/MEK/ERK pathway (47). As the FAK is a major downstream kinase of integrins we were interested if activating phosphorylations of the FAK changed due to archazolid treatment. As shown in Figure 18A archazolid treated, floating T24 cells showed reduced phosphorylation of FAK in the total cell lysate after 24h and 48h of treatment. Noteworthy, control cells detached for 24h and 48h show a strong phosphorylation of FAK.

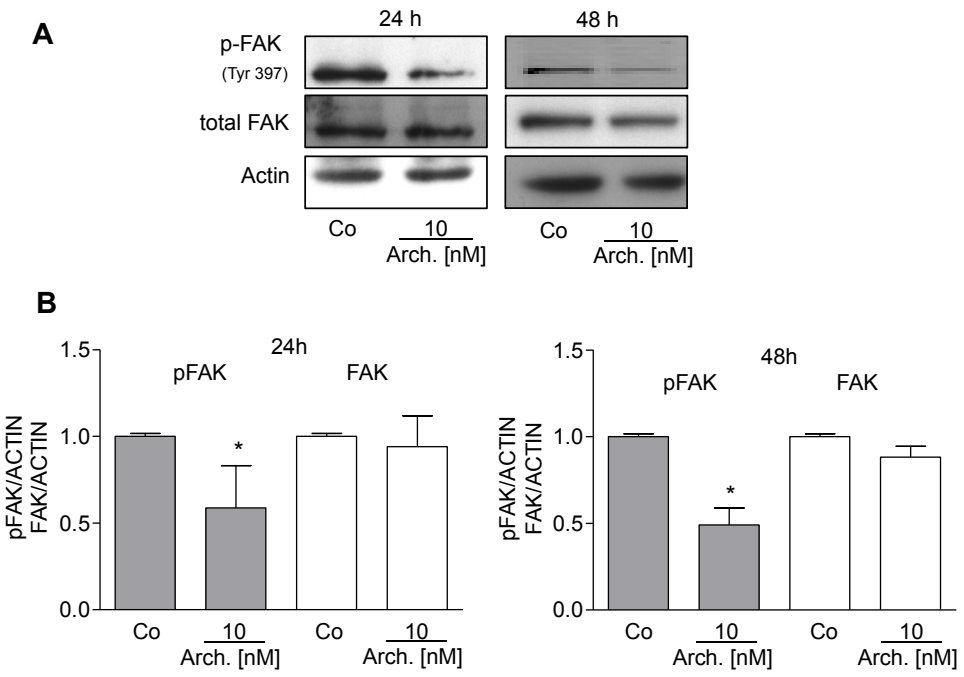

Figure 18: Archazolid treatment impairs FAK phosphorylation
A: The phosphorylation state of FAK after archazolid treatment (24h and 48h, T24 cells) is shown by Western blot **(B)** with the corresponding quantification of three independent experiments.
*P<0.05, n=3

3.3.3 Archazolid Induces Activation of Caspase-8 and Downregulation of c-FLIP

To further reveal the mechanisms of anoikis induction by archazolid, activity of caspase-8 was determined. As caspase-8 induction is a known hallmark of anoikis and the extrinsic apoptotic pathway, caspase activity was measured in cell lysates using a fluorophore generating substrate for caspase-8. Floating T24 and 4T1 cells were stimulated for 48h with different archazolid concentrations, displaying a significant increase in caspase-8 activity compared to control cells (Figure 19A). TRAIL was used as a positive control.

Moreover c-FLIP, a well-described inhibitor of caspase-8 (83) which contributes to anoikis resistance by overexpression in malignant cells (55) is reduced after 48h of treatment in floating T24 cells (Figure 19B).

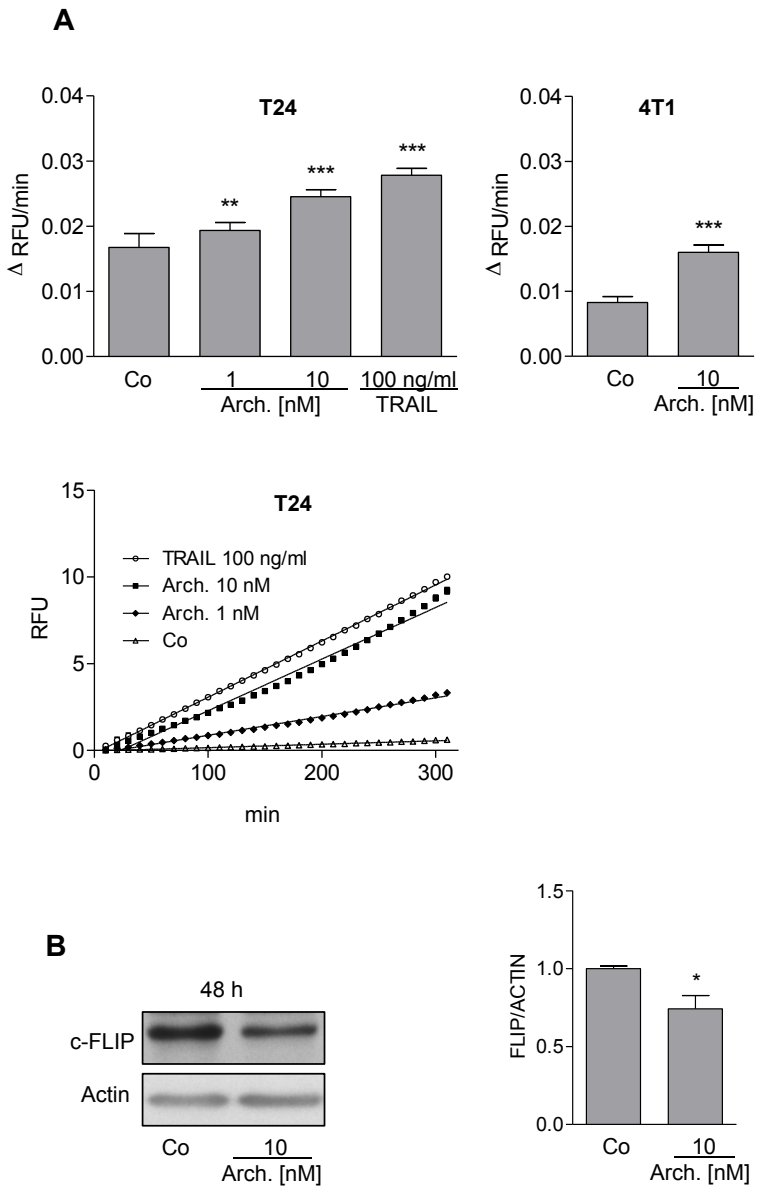

Figure 19: Activation of caspase-8 and reduction of caspase-8 inhibitor c-FLIP

A: Treated (48h) T24 and 4T1 cells were harvested and the total cell lysate was analysed for caspase-8 activity. TRAIL as a positive control was applied 1h before activity measurement. Upper panel: Evaluation of three indipendent experiments for T24 and 4T1 cells presented as relative fluorescence unit per minute (ΔRFU/min). ***P<0.001, n=3. Lower panel: Representative graph of caspase-8 activity measurement over 5h (T24 cells) displayed as relative fluorescence unit (RFU).

B: Left: The level of caspase inhibitor c-FLIP was investigated by Western blot in T24 cells after archazolid treatment (48h). Right: Quantification of three independent experiments. *P<0.01

Bars always represent the mean ± SEM of three independent experiments conducted in triplicates.

All Western blot experiments show a representative blot out of three independent experiments.

3.3.4 Archazolid Treatment Rapidly Induces BIM Translocation to Mitochondria Leading to Cytochrome C Release

As the Bcl-2 Protein BIM is considered to be the major player of the intrinsic mediated anoikis pathway (70) we analyzed BIM expression after archazolid treatment. Figure 20A indicates that cellular BIM expression is not affected by archazolid treatment for 5h, however BIM is translocated and enriched at mitochondria at early time points after archazolid exposure (i.e. 3h and 5h, T24 and 4T1 cells). Interestingly, the translocation to mitochondria is observed to be a cell type specific effect as MDA-MB-231 cells show a BIM reduction and MCF7 cells an equal level for treatment and control.

BIM localized at the mitochondrial outer membrane is responsible for Bax and Bak activation leading to the release of cytochrome C to the cytosol and subsequently to apoptosis (84). A decrease of cytochrome C in the mitochondrial fraction of T24 cells was observed after 24h and 48h of treatment (Figure 20B). Obviously both the intrinsic as well as the extrinsic pathway (Figure 19) is activated by archazolid.

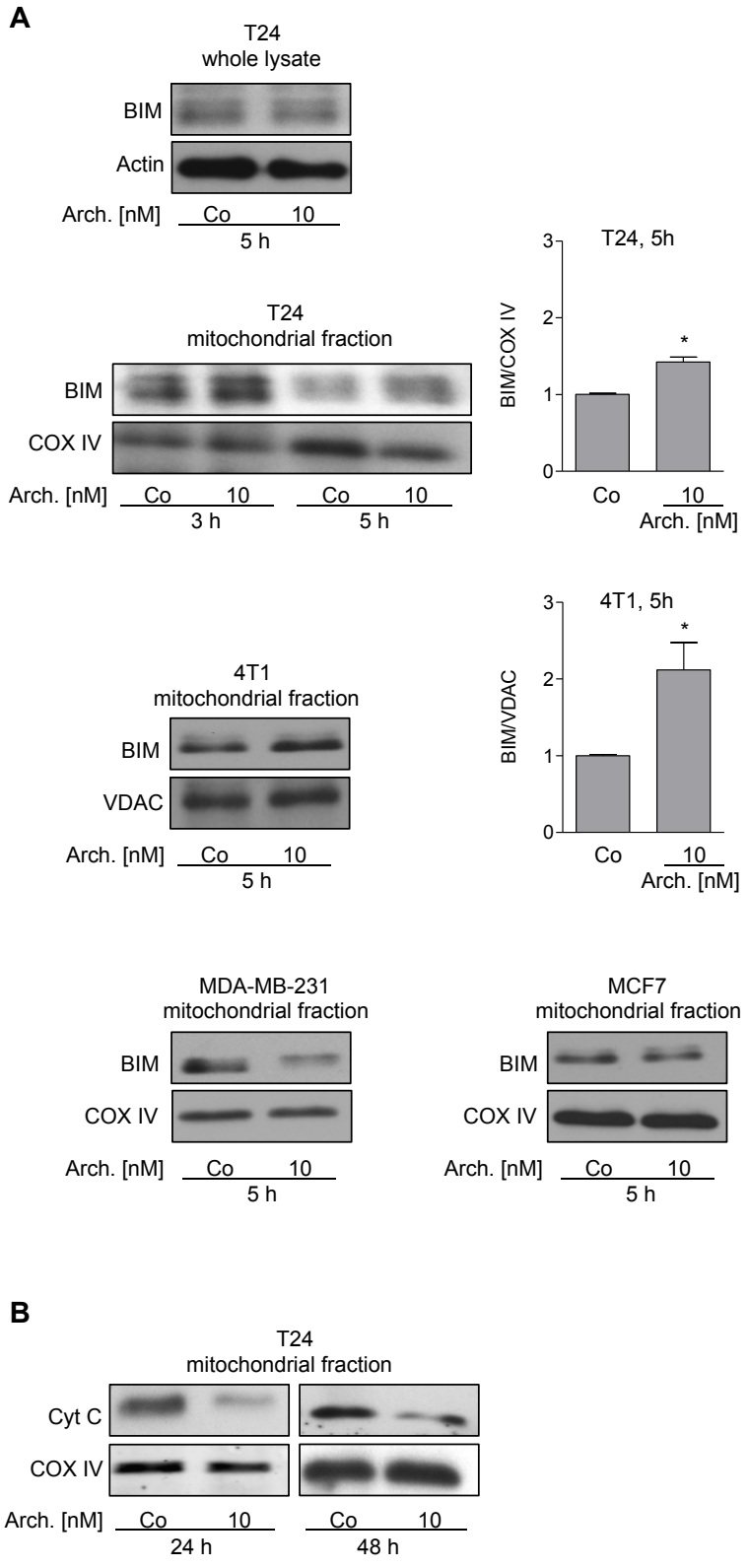

Figure 20: BIM translocation to mitochondria and cytochrome C release by archazolid

A Western blot analysis of BIM expression in whole cell lysate of untreated and archazolid treated T24 cells after 5h. BIM level was analyzed in the mitochondrial fraction of cells treated with archazolid for a few hours (3 and 5h, T24, 4T1, MDA-MB-231 and MCF7 cells). Immunoblotting for mitochondrial COX IV and VDAC was employed as control for protein loading. Quantification of multiple independent experiments was performed. *P<0.05

BIM translocates to the mitochondria in T24, and 4T1 archazolid treated cells.

B: The mitochondrial cytochrome C level after archazolid treatment (24h and 48h) is shown by Western blot analysis of mitochondrial protein of T24 cells. COX IV immunoblotting served as loading control.

Cytochrome C decreases in the mitochondrial fraction of T24, treated cells.

All blots show a representative blot out of three independent experiments.

3.4 Archazolid Triggers Mechanisms Opposing Anoikis

Chemoresistance is a major challenge in tumor therapy.
Anoikis challenges tumor cells to develop elaborated survival strategies leading to anoikis resistance. Nevertheless, additional chemoresistance strategies can generate highly metastatic cancer phenotypes. Elucidating these strategies can help to develop functional combination therapies.

Archazolid treatment triggered survival mechanisms in anoikis resistant cancer cells like a strong degradation of the pro-apoptotic protein BIM and a beneficial increase in reactive oxygen species, which can function as pro-survival second messengers.
Therefore, BIM degradation was more deeply investigated and a combinatory approach by using drugs inhibiting BIM degradation as well as ROS induction together with archazolid was tested.

3.4.1 BIM Degradation after Prolonged Treatment

Sustained exposure of detached cells to archazolid results in a strong reduction of the proapoptotic molecule BIM (Figure 21A), which is due to proteasomal degradation shown by the use of two proteasome inhibitors (MG-132 and bortezomib) (Figure 21B).

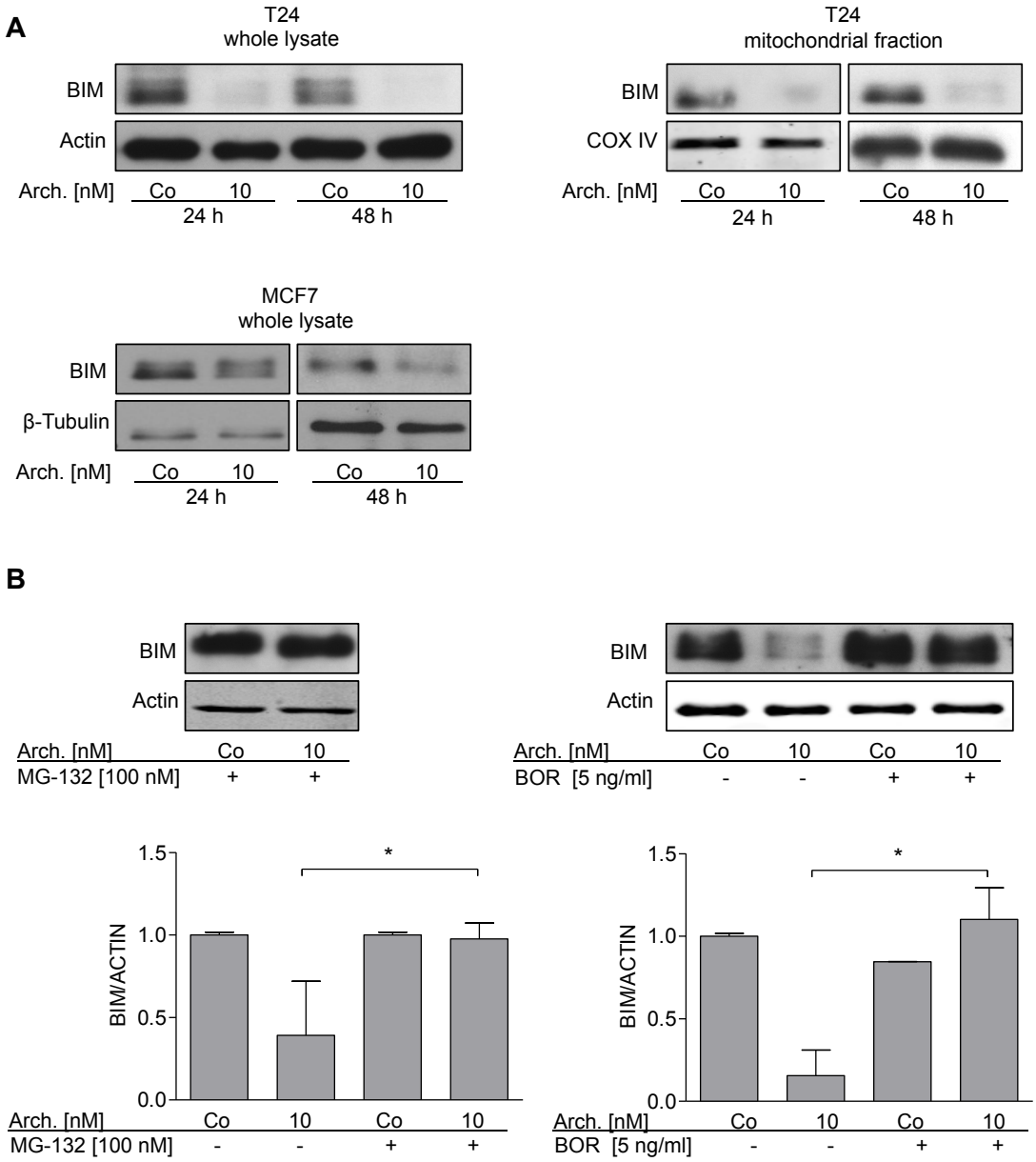

Figure 21: BIM degradation after prolonged archazolid treatment and rescue with proteasome inhibitors

A BIM degradation: BIM protein level in whole cell lysate and mitochondrial fraction after prolonged treatment with archazolid (24h, 48h) was analyzed by Western blot. Actin, COX IV and β-Tubulin were used as loading control.

B BIM rescue: A combination of archazolid (10nM) with proteasome inhibitor MG-132 (24h) (left) or bortezomib (BOR, 48h) (right) was used to investigate changes in BIM protein level by Western blot in T24 cells. The combination was applied simultaneously to the cells at time of detachment. Three independent experiments were quantified using Image J software. *P<0.05

3.4.2 Targeting BIM Degradation by Proteasome Inhibitors to Increase Cell Death Induction

Combination of archazolid with the proteasome inhibitors MG-132 (100nM) and bortezomib (5ng/ml) induced significantly higher apoptosis rates synergistically induced in T24 cells (Figure 22) and rescued BIM from degradation as shown in Figure 21B.

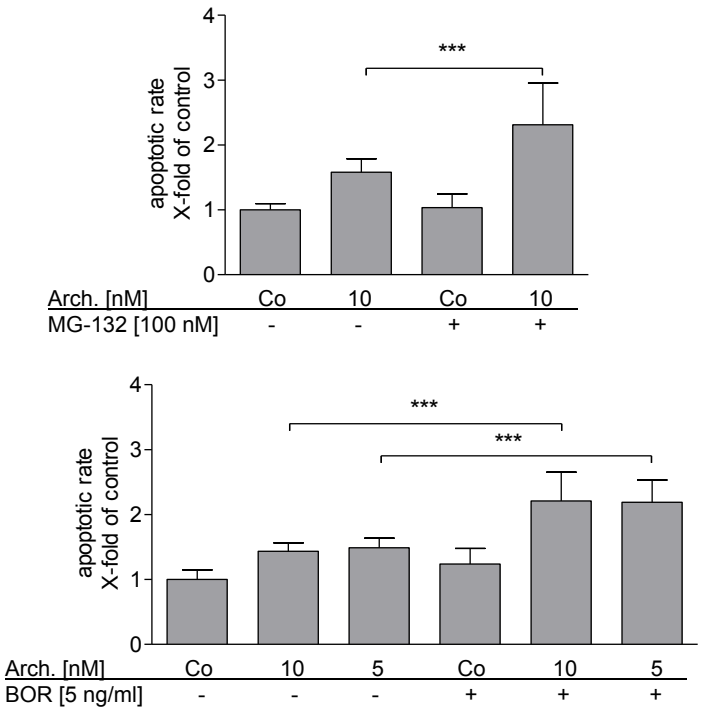

Figure 22: Inhibition of the proteasome triggers archazolid induced anoikis
Floating T24 cells were either treated with archazolid (10nM, 48h) alone or in combination with the proteasome inhibitor MG-132 or bortezomib (BOR) for. Subsequently, apoptosis induction was determined as described in materials and methods. ***P<0.001

3.4.3 Moderate ROS Induction after Archazolid Treatment as Pro-Survival Strategy to Circumvent Anoikis

Reactive oxygen species are discussed to play a major role in anoikis protection, as they can function as second messenger activating pro-survival kinases (50,51,85).

Intracellular ROS were analyzed by flow cytometry. A fluorescent dye converted by ROS was added to the cells for 30min, 37°C.

Interestingly, archazolid treatment increased ROS level significantly after 16 to 48h (Figure 23 and Figure 24) compared to floating control cells. Archazolid treated cells reach ROS levels of adherent control cells indicating a non-toxic level of ROS, as ROS can also function as second messenger activating pro-survival signals also involved in BIM regulation and degradation. This is considered one of the anoikis escape strategies used by invasive tumor cells (50,52).

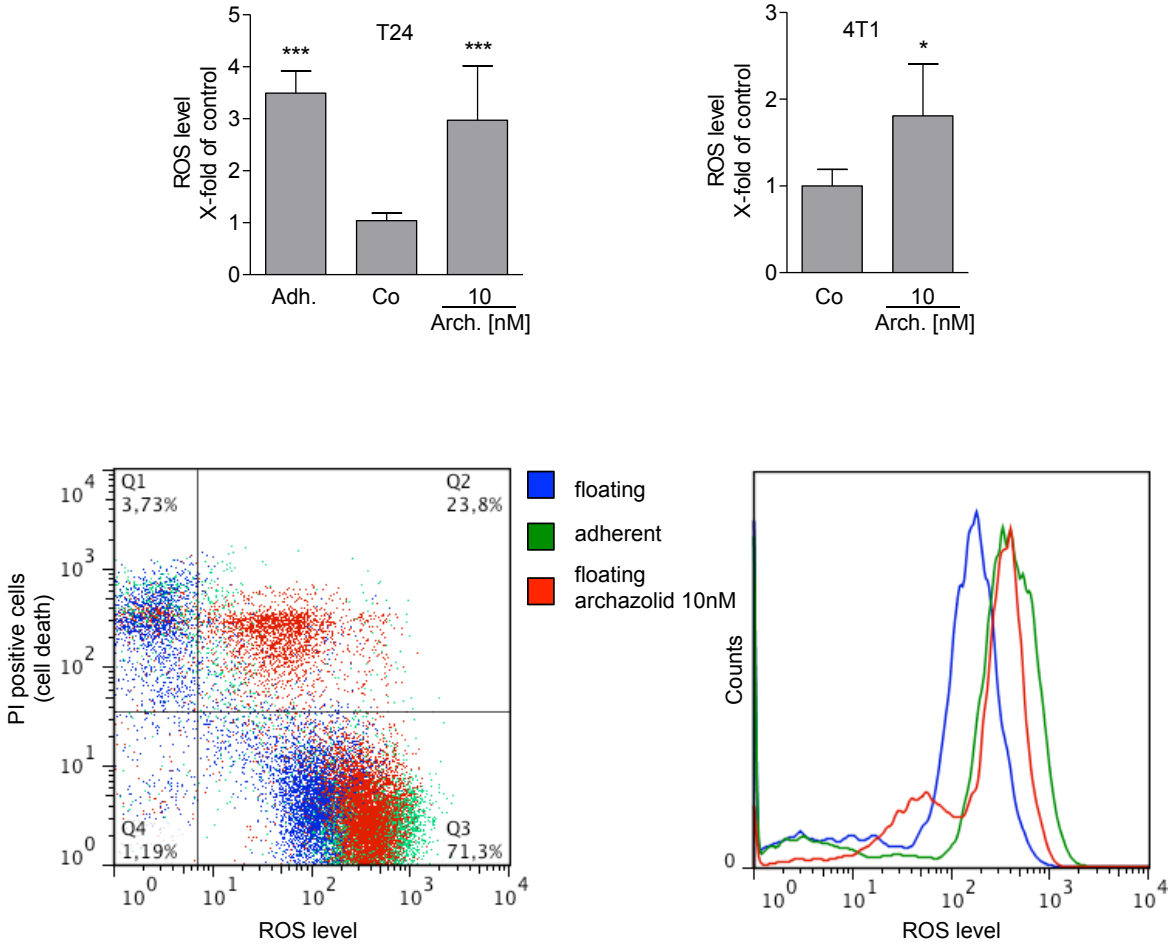

Figure 23: Beneficial ROS generation by archazolid treatment

Upper panel: Archazolid induces generation of ROS in T24 cells after 24h and in 4T1 cells after 16h of treatment. ROS generation was measured as indicated in materials and methods. Bars represent the mean ± SEM of three independent experiments conducted in triplicates. ***P<0.001, *P<0.05.

Lower panel: One representative graph of a simultaneous PI (cell death) and ROS measurement in T24 cells displayed as dotplot and the corresponding histogram.

Inhibition of ROS generation by the antioxidant N-Acetyl-L-Cystein (NAC) (Figure 24A, left) rescues BIM from proteasomal degradation induced by archazolid alone (Figure 24B) confirming the involvement of ROS in BIM degradation. NAC as well was able to increase cell death in combination with archazolid (Figure 24A right) suggesting a role for ROS in anoikis induction and inhibition.

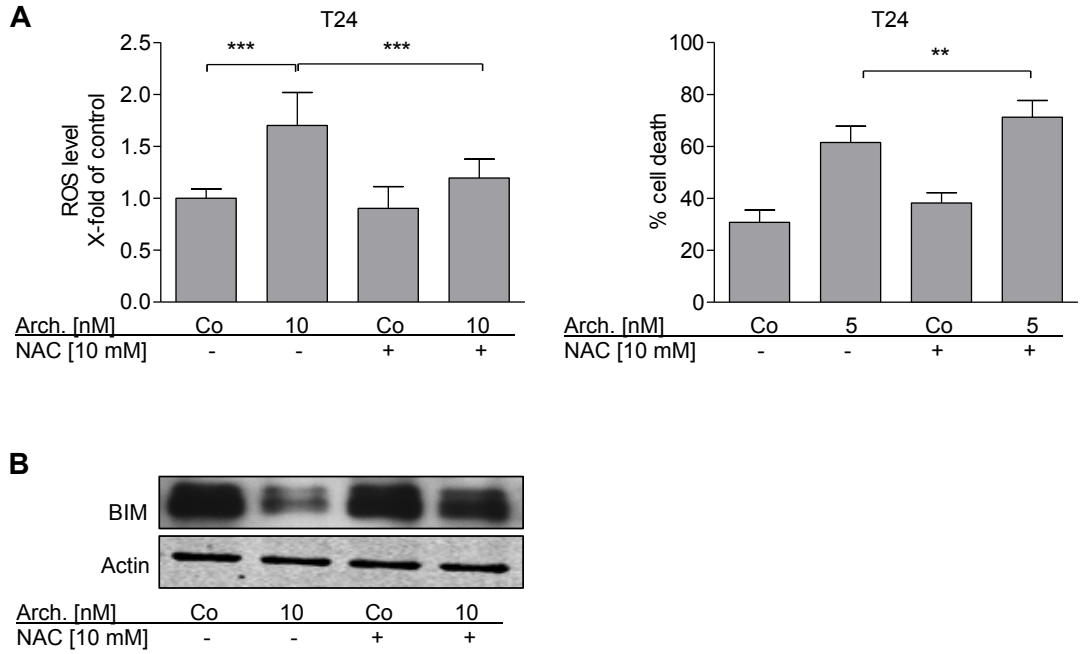

Figure 24: BIM rescue by ROS inhibition

A: Left: Archazolid induces generation of ROS, which can be inhibited by the antioxidant NAC after 48h of treatment. ROS generation was measured as indicated in materials and methods. ***P<0.001

Right: Detached T24 cells were treated with archazolid (5nM) alone or in combination with NAC (10mM) for 48h. Induction of apoptosis was measured by PI staining and flow cytometry. **P<0.01

Bars represent the mean ± SEM of three independent experiments conducted in triplicates.. **B:** ROS generation is involved in BIM degradation by archazolid. Western blot analysis showed that ROS scavenger in combination with archazolid (24h) rescued the degradation of BIM.

One representative blot out of three independent experiments is shown.

3.4.4 Kinase-Involvement in Anoikis Resistance

Additionally, kinases involved in anoikis resistance (Akt, ERK, c-Src) were affected by detachment of T24 cells showing an early increases of their phosphorylation, whereas phosphorylation of c-Src kinase was unchanged. Akt and ERK are therefore mainly responsible for activating anoikis resistance after detachment. At a later time point the phosphorylation of Akt and ERK decreased again indicating a restored balance of pro-survival and pro-apoptotic signaling (Figure 25).

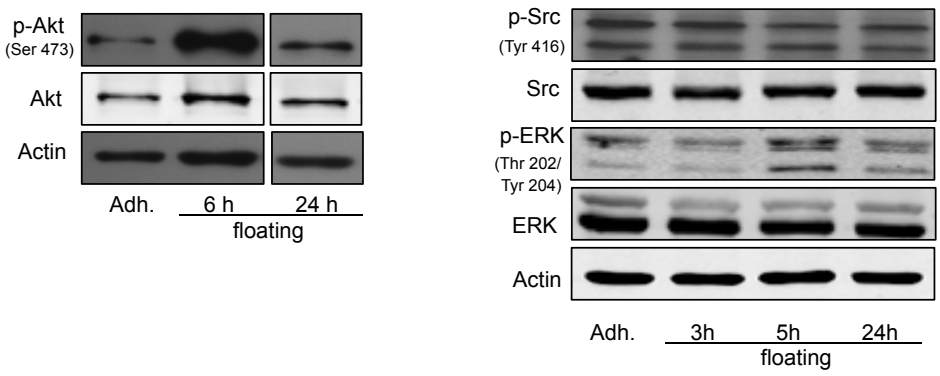

Figure 25: Phosphorylation of Akt and ERK is increased early after detachment but decreased again after 24h

Left: T24 cells were kept in suspension for 6h and 24h and compared to adherent cells. Phosphorylation of Akt was analyzed by Western blot. Actin served as loading control. One representative blot out of three independent experiments is shown.

Right: T24 cells were kept in suspension for 3, 5h and 24h in comparison to adherent cells. Phosphorylation of ERK and c-Src was analyzed by Western blot. Actin served as loading control. One representative blot out of three independent experiments is shown.

To further investigate the impact archazolid has on Akt, ERK and c-Src phosphorylation, floating, treated T24 cells were examined by Western blot analysis for the indicated phosphorylations.

Treatment of floating cells with archazolid (10nM, 48h) even further increased the phosphorylation of Akt compared to untreated control cells. The phosphorylation of ERK (48h) and c-Src (48h) did not change due to archazolid treatment (Figure 26), together suggesting archazolid induced counter mechanisms.

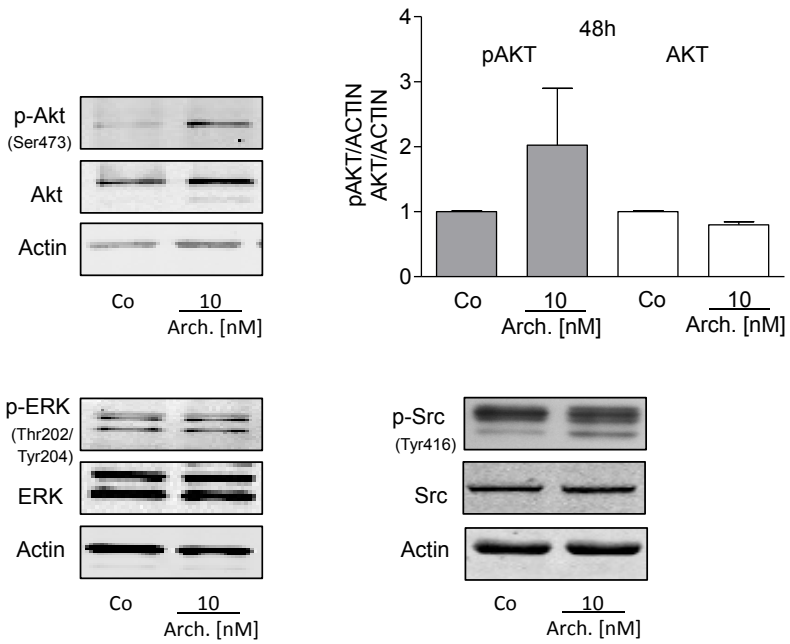

Figure 26: Influence of archazolid treatment on Akt, ERK and c-Src phosphorylation

Activation of Akt, ERK and c-Src kinases by archazolid treatment was investigated after 48h for Akt and ERK and after 24h for c-Src using Western blot analysis of their phosphorylated sites. All Western blot experiments show a representative blot out of three independent experiments. For Akt kinase activation two independent experiments were quantifies using Imaje J software.

All experiments were performed with T24 cells.

To more deeply elucidate the role of Akt, ERK and c-Src kinases, inhibitors of these proteins were used and the effect on apoptosis induction and BIM level was analyzed.

Employing specific inhibitors (LY 294002 (Akt), PD 98059 (ERK) and Saracatinib (c-Src)) led to apoptosis and prevented the decrease of BIM in archazolid treated cells (Figure 27).

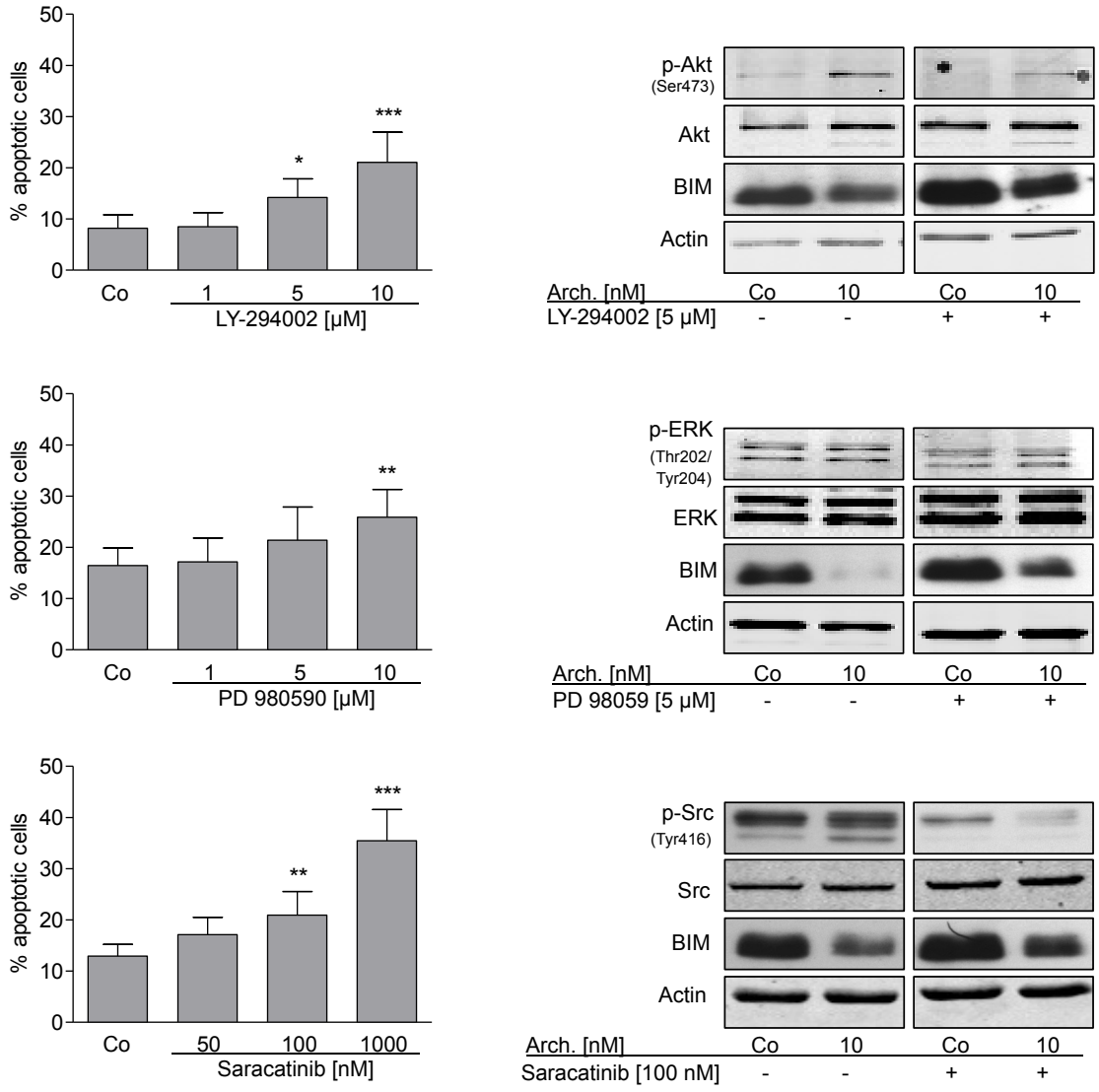

Figure 27: Inhibition of Akt, ERK and c-Src induces anoikis and rescues BIM

Left panel: Floating T24 cells were treated with Akt-, ERK-, and c-Src-inhibitors for 48h and apoptotic cell death was analyzed. Bars represent the percantage of apoptotic cells of the whole population in mean ± SEM of three independent experiments conducted in triplicates. ***P<0.001, **P<0.01, *P<0.05.

Right panel: Application of inhibitors i.e. LY 294002 (Akt), PD 98059 (ERK) or Saracatinib (c-Src) together with archazolid were used to analyse changes in BIM protein level. Changes of Akt and ERK were investigated after 48h and of c-Src after 24h.

All Western blot experiments show a representative blot out of three independent experiments. All experiments were performed with T24 cells

DISCUSSION

4 DISCUSSION

This work disclosed that pharmacological inhibition of V-ATPase by archazolid induces anoikis in invasive cancer cells, which contributes to the distinct anti-metastatic action of archazolid *in vivo*. Thus we could add important new information regarding the role of V-ATPase in cancer dissemination.

4.1 The V-ATPase in Cancer Cells

Up to now it has been reported that the abundance of V-ATPase on the plasma membrane of tumor cells correlates with their invasiveness. Several well-known V-ATPase inhibitors like concanamycin and bafilomycin were shown to lead to growth arrest and cell death induction in a variety of tumor cells (2,86,87). Also the newly developed V-ATPase inhibitors salicylihalamide (88) and NIK-12192 (89) have demonstrated anti-tumor activity although the exact molecular mechanisms of V-ATPase inhibitors leading to inhibition of tumor cell invasion remain to be elucidated. Cell surface located V-ATPase is hypothesized to create a proton efflux leading to an acidic pericellular microenvironment that promotes the activity of pro-invasive proteases and/or rescues tumor cells from intracellular acidification due to increased glycolysis, which can otherwise lead to apoptosis (8,90). However, evidence accumulates that the endolysosomal V-ATPase is important as antitumoral/antimetastatic target. Recent work in our group showed that V-ATPase inhibition by archazolid impairs endocytotic traffic of migratory signaling molecules such as Rac1 and EGF-R, which is pivotal for directed and polarized cell movements (40). Abrogation of endosomal trafficking by V-ATPase inhibition was reported to also have impact on tumor growth and apoptosis induction suppressing activation of important signaling molecules such as Rab27B or activation of caspase-8 (91,92).

We showed that V-ATPase inhibition influences anoikis resistance in invasive cancer cells by triggering anoikis pathways and impairing survival-receptor signaling. This, presumably by inhibition of the endolysosomal V-ATPase, as receptor recycling and autophagy play important roles in anoikis induction and resistance.

4.2 Relevance of Anoikis in Normal and Malignant Cells

This work using archazolid as a tool to inhibit V-ATPase provides important information on regulation of anoikis and especially anoikis resistance in cancer.

From a physiological point of view, anoikis is an important mechanism to remove cells, which are currently not in their correct location, lacking a correct adhesion and thus guaranteeing tissue homeostasis and preventing dysplastic growth. In other words most cell types need proper cell-cell and cell-matrix interactions to survive. Cell to ECM interactions occur mainly via specific integrins and trigger a cascade of pro-survival and proliferative signals (47,52).

Metastatic cancer cells in contrast to non-malignant tissue cells, do not require adhesion to the ECM to survive and proliferate, they are mostly insensitive to anoikis and in fact resistance to anoikis is a key regulator for tumor cell invasion and metastasis (52) (Figure 28). Tumor cells use various strategies to acquire anoikis resistance such as the constitutive activation of survival pathways (PI3K/Akt, MEK/ERK and c-Src family kinases), alteration of the integrin expression pattern or generation of oxidative stress and inhibition of apoptotic pathways (50,52,55,93).

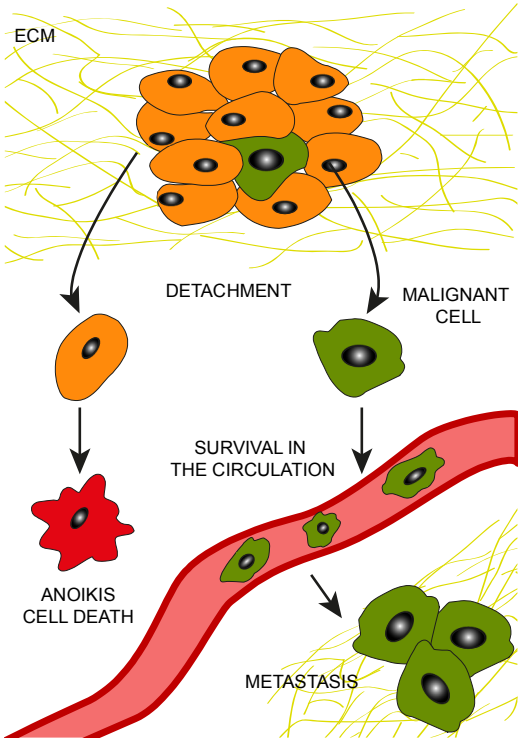

Figure 28: Anoikis resistance as prerequisite for tumor cell metastasis
Normal tissue cells are programmed to anoikis when detached from their respective ECM. Malignant cells can acquire anoikis resistance by several strategies to survive in the circulation. This is a precondition to form metastases in distant tissues or organs.

4.3 Anoikis Induction by Archazolid a V-ATPase Inhibitor

How a V-ATPase inhibitor could possibly affect anoikis induction in invasive cancer cells is a challenging issue to solve. It is known that detachment can induce autophagy as a survival mechanism preventing anoikis. Inhibition of autophagy increased caspase-3 activity in detached cells (72) and BIM was thought to influence autophagy by interacting with beclin-1 and inhibiting autophagosome formation (73). It has been shown that integrin β1 inhibition directly correlates with autophagy induction suggesting an important role in anoikis (74). V-ATPase inhibition on the other hand is known to block late stages of autophagy due to alkalization of lysosomes and thereby inhibiting protein degradation in autolysosomes. Archazolid is a very potent V-ATPase inhibitor alkalizing cell-compartments within hours as shown in Figure 9. Treatment of different adherent cancer cell lines led to reduced lysosome acidification already after 2-4h indicating an early stop of protein degradation, depriving anoikis resistant cells of this escape mechanism.

V-ATPase inhibition might also affect integrin signaling as integrin activities are dependent on fast endocytosis rates and V-ATPase regulates receptor recycling via acidification of endosomes and lysosomes (3,94,95). It is known, that block of endosome acidification leads to trafficking inhibition probably because of a general block in the formation of carriers important for the formation of clathrin-coated-vesicles (CCV) (94). CCV formation is the major endocytotic pathway in mammalian cells (96). Also an accumulation of receptors on the cell surface due to blocked internalization is a reported effect of V-ATPase inhibition (40,94,97).

That is why it has been hypothesized that V-ATPase inhibition affects anoikis induction as receptor recycling is attenuated consequently influencing membrane receptor signaling.

In fact, we could show that archazolid induces anoikis in invasive urinary and breast cancer cells. Anoikis is provoked by a reduction of active integrin ß1 on the cell surface, an activation of caspase-8 and an early translocation of BIM to the mitochondria followed by release of cytochrome C. Of note, archazolid treated breast tumor cells injected (i.v.) in mice showed a reduced formation of lung metastasis (Figure 16). This study further identified counter mechanisms induced by archazolid treatment like a strong proteasomal downregulation of BIM provoked by generation of ROS and active pro-survival kinases.

4.3.1 Impaired Adhesion after Archazolid Treatment

As integrins function as the main cellular receptors for ECM-cell interactions they are assembled in specific adhesive structures like focal adhesions, which directly link the cytoskeleton to the ECM. In mature focal adhesions integrins are in an active conformation and constantly ligand-

bound (98). Integrin-ECM interactions stimulate focal adhesion formation functioning as a signaling hub by accumulating multiple kinases and scaffold proteins (99). Hence, impaired adhesion as seen by archazolid (Figure 10) pretreatment implies a reduced functionality of focal adhesions. This assumption was strengthened as staining of vinculin by a fluorescent antibody and visualization by confocal microscopy revealed that archazolid treatment altered vinculin incidence and localization (Figure 11). Vinculin is a major structural protein in the focal adhesions and often used as focal adhesion marker (100,101). The images showed that after treatment vinculin clustering at the periphery of the cells was reduced. Archazolid treated cells develop more spike-like focal adhesions, likely to compensate for a reduced functionality proved by the adhesion assay. As reduced adhesion ability might trigger enhanced focal adhesion formation to level up the output.

4.3.2 Archazolid Induces Cell Death in Anoikis Resistant Cancer Cells by Distinct Activation of Apoptotic Pathways

In experimental anoikis models, cells are forced to grow anchorage independent, which triggers the above-mentioned stress and survival responses leading to a selection of the "fittest" seen by an elevated apoptosis level of floating cells compared to adherent ones (Figure 14). There are reports that an oncogenic epithelial-mesenchymal transition (EMT) also is characterized by anoikis resistance. EMT is a process normally occurring during development forming the primary mesenchyme. Epithelial cells undergoing EMT loose the necessity of attachment for their survival, acquire more motility, change their morphology and their repertoire of adhesion molecules such as E-catherin and additionally silence epithelium-specific genes and activate mesenchymal-specific genes. It has been shown that a subgroup of breast cancer cell lines with especially invasive properties had mostly mesenchymal gene-expression signatures compared to more luminal like cell lines (102–104). Evidently, there is a close relationship between oncogenic EMT and acquisition of anoikis resistance. We could demonstrate, that on the one hand cell death slightly increases by detachment and on the other hand anoikis resistance is activated by Akt and ERK induction (Figure 25). Taking this into account it would be very interesting to further investigate if an EMT like process occurs in our cell lines during extended detachment.

Anoikis resistance is often accompanied by resistance to chemotherapeutics, supported by our observation that adherent cancer cells are significantly more sensitive to archazolid then detached cells (Figure 15). ECM/integrin signaling can protect cancer cells from drug induced apoptosis by activation of the Akt and ERK signaling pathway (63).

The clear effect of archazolid on anchorage independent growth of cancer cells as well as the induction of cell death in cells forced to stay detached is thus remarkable (Figure 12 and Figure 13). Even more so having learned that archazolid treatment itself potently induces anoikis resistance via ROS generation and activation of Akt, which together with constitutive active ERK and c-Src leads to the removal of BIM, which will be further discussed in the next sections (Figure 23, Figure 26 and Figure 27).

Obviously, it is important to find out how a compound like archazolid finally achieves anoikis induction, meaning, which pathways are involved.

Anoikis is characterized as an apoptotic cell death executed by features of the intrinsic and extrinsic apoptotic pathway and the loss of survival signals by unligated anchorage proteins like integrins (75). The extrinsic pathway is initiated by caspase-8 activating effector caspases or promoting mitochondrial cytochrome C release (75,105).

Archazolid evidently uses the extrinsic apoptotic pathway as shown by a downregulation of c-FLIP and a distinct caspase-8 activation (Figure 19). Recruitment of caspase-8 and its activation has been shown to occur by loss of anchorage to ECM and unligated integrins (53,106). Integrins with the β1 subunit in common are the major receptors for ECM components responsible for cell-ECM interactions (47). Interestingly, cell surface β1 integrin of cancer cells, floating for 24h was still as active as in adherent cells, suggesting an inside-out integrin activation supporting anoikis resistance of these cells (107). Importantly, archazolid reduced the amount of active integrin β1 on the cell surface leaving the total integrin level constant probably through an altered receptor recycling (Figure 17).

4.3.3 Impacts on the Integrin Downstream Signaling by Archazolid Treatment

In consequence, downstream pro-survival signals like the phosphorylation of one key player in anoikis protection, FAK (82) was affected by archazolid treatment (Figure 18). FAK together with c-Src then interact with numerous molecules recruiting and activating other pro-survival proteins like PI3K/Akt or ERK (46). We observed that T24 cells, shortly after detachment (5h) induce anoikis resistance by activating Akt and ERK which decreases when cells were detached for 24h suggesting a restored balance between apoptotic and survival players. For c-Src kinase the phosphorylation was not changed due to detachment over 3, 5 and 24h compared to adherent control cells implying no direct involvement in the immediate anoikis resistance (Figure 25).

Unexpectedly, we did not observe inhibitory effects of archazolid on either Akt, ERK or c-Src but an activation of Akt which is considered to be part of the counter, pro-survival mechanism induced by archazolid (Figure 26).

4.3.4 BIM: First Activated then Inhibited by Archazolid Treatment

Anoikis due to the intrinsic pathway is mainly initiated by BIM (108). BIM, a member of the Bcl-2 family activates Bax and Bak which leads to the permeabilisation of the outer mitochondrial membrane and the release of cytochrome C to the cytosol thereby activating a caspase cascade inducing cell death (60,84). In fact, BIM has been reviewed as a potential target for tumor therapy as BIM promotes anoikis in many tumor cell types and BIM suppression supports metastasis and chemoresistance (70). BIM regulation is dependent on cell surface molecules like integrins and the epidermal growth factor receptor (EGFR) (54).

We found that BIM was rapidly translocated to the mitochondria by archazolid treatment followed by cytochrome C release (Figure 20) pointing to an involvement of the intrinsic apoptotic pathway.

4.4 Resistance Mechanisms after Archazolid Treatment

Of note BIM inhibition seems to be also the major factor used by T24 and MCF 7 cells to induce resistance to anoikis as BIM gets strongly degraded at a later time of archazolid exposure (Figure 21A). In MDA-MB-231 cells, a highly invasive breast cancer cell line, this degradation could even be observed shortly after archazolid treatment in detached cells (Figure 20) indicating that the ability to control BIM is connected to the metastatic potential. The fact that rescue of BIM degradation (Figure 21B) employing proteasome inhibitors MG-132 and bortezomib synergistically increased archazolid induced cell death underscores the important role of this BH-3 only protein in the regulation of anoikis and its failure (Figure 22).

As kinases such as ERK, Akt and c-Src are known to regulate BIM degradation and expression it was tempting to employ specific kinase inhibitors in order to gain further insight in the archazolid triggered BIM removal and thus chemoresistance (109). Akt and ERK can both phosphorylate BIM to be proteasomal degraded or sequestered, thereby having an immediate effect on BIM clearance in the cytosol (58,109). The relevance of these kinases in survival was shown by the fact that kinase inhibitors alone at high concentration induce anoikis. Co-stimulation of archazolid with moderate concentrations of kinase inhibitors rescued BIM, indicating that cells actively block BIM activation by various pathways in response to archazolid treatment (Figure 27). This

further underlines the highly efficient survival and anoikis resistance mechanisms of invasive tumor cells and highlights compounds such as archazolid still inducing cell death.

Additionally, ROS are considered critical players in anoikis resistance. Integrin mediated adhesion induces a transient burst of high ROS levels transducing survival signals by activation of c-Src kinases. Activated c-Src kinases trans-phosphorylate EGF-receptor ligands, activating ERK and PI3K/Akt pathways. Scavenging of ROS in adherent cells leads to BIM induction and cell death (50,51). ROS are also recognized as second messenger in cell growth, proliferation, adhesion and cell spreading in untransformed cells (110). Induction of ROS in tumor cells is correlated to tumor initiation and progression as well as with tumor invasiveness (111). Anoikis sensitive cells show decreased ROS levels after detachment correlating with cell death induction (50). Now, we discovered that archazolid treatment of floating cells resulted in elevated ROS levels compared to untreated cells, but did not exceed the steady state level of ROS in untreated adherent cells (Figure 23). Still, cell death was induced by archazolid. This elevated ROS could be a further explanation for the prominent removal of BIM protein. We showed, in accordance to Giannoni et al. (50) that co-treatment of archazolid with a ROS scavenger led to increased cell death and increased BIM levels (Figure 24). Therefore, ROS must play a critical role in resistance to archazolid-induced anoikis.

4.5 Conclusion and Outlook

This study demonstrates that archazolid induces anoikis in highly invasive tumor cells by activation of the extrinsic and intrinsic apoptotic pathway. Anoikis induction is accompanied by initiation of highly productive resistance mechanisms especially removal of BIM by activation of Akt and induction of ROS. Understanding the mode of actions leading to cell death by archazolid treatment and the challenges of counter reactions can help gaining deeper insight in anoikis resistance mechanisms, chemoresistance and the metastatic transition of detached tumor cells.

A clear characterization of anoikis resistance mechanisms depending on tumor cell type, drug treatment, EMT occurence and metastatic potential is therefore desirable to adjust chemotherapies or apply suitable combination drug therapies as metastasis is still the number one cause for death by cancer.

REFERENCES

5 REFERENCES

1. Forgac M. Structure, function and regulation of the vacuolar (H+)-ATPases. FEBS Lett. 1998;440:258–63.
2. Forgac M. Vacuolar ATPases: rotary proton pumps in physiology and pathophysiology. Nat. Rev. Mol. Cell Biol. 2007;8:917–29.
3. Hinton A, Bond S, Forgac M. V-ATPase functions in normal and disease processes. Pflugers Arch. 2009;457:589–98.
4. Cross RL, Müller V. The evolution of A-, F-, and V-type ATP synthases and ATPases: reversals in function and changes in the H+/ATP coupling ratio. FEBS Lett. 2004;576:1–4.
5. Yoshida M, Muneyuki E, Hisabori T. ATP synthase--a marvellous rotary engine of the cell. Nat. Rev. Mol. Cell Biol. 2001;2:669–77.
6. Martinez-Zaguilan R, Lynch RM, Martinez GM, Gillies RJ. Vacuolar-type H(+)-ATPases are functionally expressed in plasma membranes of human tumor cells. Am. J. Physiol. 1993;265:C1015–29.
7. Sennoune SR, Luo D, Martínez-Zaguilán R. Plasmalemmal vacuolar-type H+-ATPase in cancer biology. Cell Biochem. Biophys. 2004;40:185–206.
8. Sennoune SR, Bakunts K, Martínez GM, Chua-Tuan JL, Kebir Y, Attaya MN, et al. Vacuolar H+-ATPase in human breast cancer cells with distinct metastatic potential: distribution and functional activity. Am. J. Physiol. Cell Physiol. 2004;286:C1443–52.
9. Pérez-Sayáns M, García A. V-ATPase Inhibitors in Cancer Treatment and Their Implication in Multidrug Resistance in Oral Squamous Cell Carcinoma. Curr. Cancer Treat. - Nov. Beyond Conv. Approaches. InTech; 2011.
10. Gatenby R a, Gillies RJ. Why do cancers have high aerobic glycolysis? Nat. Rev. Cancer. 2004;4:891–9.
11. Barar J, Omidi Y. Dysregulated pH in Tumor Microenvironment Checkmates Cancer Therapy. Bioimpacts. 2013;3:149–62.
12. Lu Q, Lu S, Huang L, Wang T, Wan Y, Zhou CX, et al. The expression of V-ATPase is associated with drug resistance and pathology of non-small-cell lung cancer. Diagn. Pathol. Diagnostic Pathology; 2013;8:145.
13. Fogarty FM, O'Keeffe J, Zhadanov A, Papkovsky D, Ayllon V, O'Connor R. HRG-1 enhances cancer cell invasive potential and couples glucose metabolism to cytosolic/extracellular pH gradient regulation by the vacuolar-H(+) ATPase. Oncogene. 2013;
14. Torigoe T, Izumi H, Ishiguchi H, Uramoto H, Murakami T, Ise T, et al. Enhanced expression of the human vacuolar H+-ATPase c subunit gene (ATP6L) in response to anticancer agents. J. Biol. Chem. 2002;277:36534–43.
15. Werner G, Hagenmaier H, Drautz H, Baumgartner A, Zähner H. Metabolic products of microorganisms. 224. Bafilomycins, a new group of macrolide antibiotics. Production, isolation, chemical structure and biological activity. J. Antibiot. (Tokyo). 1984;37:110–7.
16. Kinashi H, Someno K, Sakaguchi K. Isolation and characterization of concanamycins A, B and C. J. Antibiot. (Tokyo). 1984;37:1333–43.
17. Kinashi H, Sakaguchi K, Higashijima T, Miyazawa T. Structures of concanamycins B and C. J. Antibiot. (Tokyo). 1982;35:1618–20.

18. Bowman EJ, Siebers A, Altendorf K. Bafilomycins: a class of inhibitors of membrane ATPases from microorganisms, animal cells, and plant cells. Proc. Natl. Acad. Sci. U. S. A. 1988;85:7972–6.
19. Dröse S, Bindseil KU, Bowman EJ, Siebers A, Zeeck A, Altendorf K. Inhibitory effect of modified bafilomycins and concanamycins on P- and V-type adenosinetriphosphatases. Biochemistry. 1993;32:3902–6.
20. Dröse S, Altendorf K. Bafilomycins and concanamycins as inhibitors of V-ATPases and P-ATPases. J. Exp. Biol. 1997;200:1–8.
21. Zhang J, Feng Y, Forgac M. Proton conduction and bafilomycin binding by the V0 domain of the coated vesicle V-ATPase. J. Biol. Chem. 1994;269:23518–23.
22. Crider BP, Xie XS, Stone DK. Bafilomycin inhibits proton flow through the H+ channel of vacuolar proton pumps. J. Biol. Chem. 1994;269:17379–81.
23. Bowman BJ, Bowman EJ. Mutations in subunit C of the vacuolar ATPase confer resistance to bafilomycin and identify a conserved antibiotic binding site. J. Biol. Chem. 2002;277:3965–72.
24. Huss M, Ingenhorst G, König S, Gassel M, Dröse S, Zeeck A, et al. Concanamycin A, the specific inhibitor of V-ATPases, binds to the V(o) subunit c. J. Biol. Chem. 2002;277:40544–8.
25. Bowman EJ, Graham L a, Stevens TH, Bowman BJ. The bafilomycin/concanamycin binding site in subunit c of the V-ATPases from Neurospora crassa and Saccharomyces cerevisiae. J. Biol. Chem. 2004;279:33131–8.
26. Boyd MR, Farina C, Belfiore P, Gagliardi S, Kim JW, Hayakawa Y, et al. Discovery of a novel antitumor benzolactone enamide class that selectively inhibits mammalian vacuolar-type (H+)-atpases. J. Pharmacol. Exp. Ther. 2001;297:114–20.
27. Huss M, Wieczorek H. Inhibitors of V-ATPases: old and new players. J. Exp. Biol. 2009;212:341–6.
28. Osteresch C, Bender T, Grond S, von Zezschwitz P, Kunze B, Jansen R, et al. The binding site of the V-ATPase inhibitor apicularen is in the vicinity of those for bafilomycin and archazolid. J. Biol. Chem. 2012;287:31866–76.
29. Gagliardi S, Nadler G, Consolandi E, Parini C, Morvan M, Legave MN, et al. 5-(5,6-Dichloro-2-indolyl)-2-methoxy-2,4-pentadienamides: novel and selective inhibitors of the vacuolar H+-ATPase of osteoclasts with bone antiresorptive activity. J. Med. Chem. 1998;41:1568–73.
30. Gagliardi S, Gatti PA, Belfiore P, Zocchetti A, Clarke GD, Farina C. Synthesis and structure-activity relationships of bafilomycin A1 derivatives as inhibitors of vacuolar H+-ATPase. J. Med. Chem. 1998;41:1883–93.
31. Páli T, Dixon N, Kee TP, Marsh D. Incorporation of the V-ATPase inhibitors concanamycin and indole pentadiene in lipid membranes. Spin-label EPR studies. Biochim. Biophys. Acta. 2004;1663:14–8.
32. Dixon N, Páli T, Kee TP, Marsh D. Spin-labelled vacuolar-ATPase inhibitors in lipid membranes. Biochim. Biophys. Acta. 2004;1665:177–83.
33. Dixon N, Páli T, Kee TP, Ball S, Harrison MA, Findlay JBC, et al. Interaction of spin-labeled inhibitors of the vacuolar H+-ATPase with the transmembrane Vo-sector. Biophys. J. 2008;94:506–14.
34. Reichenbach H, Höfle G. Biologically active secondary metabolites from myxobacteria. Biotechnol. Adv. 1993;11:219–77.
35. Sasse F, Steinmetz H, Höfle G, Reichenbach H. Archazolids, new cytotoxic macrolactones from Archangium gephyra (Myxobacteria). Production, isolation, physico-chemical and biological properties. J. Antibiot. (Tokyo). 2003;56:520–5.
36. Huss M, Sasse F, Kunze B, Jansen R, Steinmetz H, Ingenhorst G, et al. Archazolid and apicularen: novel specific V-ATPase inhibitors. BMC Biochem. 2005;6:13.

37. Bockelmann S, Menche D, Rudolph S, Bender T, Grond S, von Zezschwitz P, et al. Archazolid A Binds to the Equatorial Region of the c-Ring of the Vacuolar H+-ATPase. J. Biol. Chem. 2010;285:38304–14.
38. Roethle PA, Chen IT, Trauner D. Total synthesis of (-)-archazolid B. J. Am. Chem. Soc. 2007;129:8960–1.
39. Menche D, Hassfeld J, Li J, Mayer K, Rudolph S. Modular total synthesis of archazolid A and B. J. Org. Chem. 2009;74:7220–9.
40. Wiedmann RM, von Schwarzenberg K, Palamidessi A, Schreiner L, Kubisch R, Liebl J, et al. The V-ATPase-inhibitor archazolid abrogates tumor metastasis via inhibition of endocytic activation of the Rho-GTPase Rac1. Cancer Res. 2012;72:5976–87.
41. Von Schwarzenberg K, Wiedmann RM, Oak P, Schulz S, Zischka H, Wanner G, et al. Mode of cell death induction by pharmacological vacuolar H+-ATPase (V-ATPase) inhibition. J. Biol. Chem. 2013;288:1385–96.
42. Von Schwarzenberg K, Lajtos T, Simon L, Müller R, Vereb G, Vollmar AM. V-ATPase inhibition overcomes trastuzumab resistance in breast cancer. Mol. Oncol. 2013;
43. Mehlen P, Puisieux A. Metastasis: a question of life or death. Nat. Rev. Cancer. 2006;6:449–58.
44. Frisch SM, Francis H. Disruption of epithelial cell-matrix interactions induces apoptosis. J. Cell Biol. 1994;124:619–26.
45. Gilmore AP. Anoikis. Cell Death Differ. 2005;12 Suppl 2:1473–7.
46. Chiarugi P, Giannoni E. Anoikis: a necessary death program for anchorage-dependent cells. Biochem. Pharmacol. 2008;76:1352–64.
47. Vachon PH. Integrin signaling, cell survival, and anoikis: distinctions, differences, and differentiation. J. Signal Transduct. 2011;2011:738137.
48. Zhan M, Zhao H, Han ZC. Signalling mechanisms of anoikis. Histol. Histopathol. 2004;19:973–83.
49. Grossmann J. Molecular mechanisms of "detachment-induced apoptosis--Anoikis". Apoptosis. 2002;7:247–60.
50. Giannoni E, Buricchi F, Grimaldi G, Parri M, Cialdai F, Taddei ML, et al. Redox regulation of anoikis: reactive oxygen species as essential mediators of cell survival. Cell Death Differ. 2008;15:867–78.
51. Chiarugi P, Pani G, Giannoni E, Taddei L, Colavitti R, Raugei G, et al. Reactive oxygen species as essential mediators of cell adhesion: the oxidative inhibition of a FAK tyrosine phosphatase is required for cell adhesion. J. Cell Biol. 2003;161:933–44.
52. Kim Y, Koo KH, Sung JY, Yun U, Kim H. Anoikis Resistance : An Essential Prerequisite for Tumor Metastasis. Int. J. Cell Biol. 2012;2012:306879.
53. Frisch SM. Caspase-8: fly or die. Cancer Res. 2008;68:4491–3.
54. Reginato MJ, Mills KR, Paulus JK, Lynch DK, Sgroi DC, Debnath J, et al. Integrins and EGFR coordinately regulate the pro-apoptotic protein Bim to prevent anoikis. Nat. Cell Biol. 2003;5:733–40.
55. Simpson CD, Anyiwe K, Schimmer AD. Anoikis resistance and tumor metastasis. Cancer Lett. 2008;272:177–85.
56. Guadamillas MC, Cerezo A, Del Pozo M a. Overcoming anoikis--pathways to anchorage-independent growth in cancer. J. Cell Sci. 2011;124:3189–97.
57. Piñon JD, Labi V, Egle a, Villunger a. Bim and Bmf in tissue homeostasis and malignant disease. Oncogene. 2008;27 Suppl 1:S41–52.
58. Qi X-J, Wildey GM, Howe PH. Evidence that Ser87 of BimEL is phosphorylated by Akt and regulates BimEL apoptotic function. J. Biol. Chem. 2006;281:813–23.
59. McConkey DJ, Bondar V. Apoptosis, Senescence, and Cancer. In: Gewirtz DA, Holt SE, Grant S, editors. Totowa, NJ: Humana Press; 2007. page 109–22.

60. Kim H, Tu H-C, Ren D, Takeuchi O, Jeffers JR, Zambetti GP, et al. Stepwise activation of BAX and BAK by tBID, BIM, and PUMA initiates mitochondrial apoptosis. Mol. Cell. 2009;36:487–99.
61. Stupack DG, Puente XS, Boutsaboualoy S, Storgard CM, Cheresh D a. Apoptosis of adherent cells by recruitment of caspase-8 to unligated integrins. J. Cell Biol. 2001;155:459–70.
62. Elmore S. Apoptosis: a review of programmed cell death. Toxicol. Pathol. 2007;35:495–516.
63. Aoudjit F, Vuori K. Integrin signaling in cancer cell survival and chemoresistance. Chemother. Res. Pract. 2012;2012:283181.
64. Frisch SM, Screaton RA. Anoikis mechanisms. Curr. Opin. Cell Biol. 2001;13:555–62.
65. Giancotti FG. Integrin Signaling. Science. 1999;285:1028–33.
66. Bunek J, Kamarajan P, Kapila YL. Anoikis mediators in oral squamous cell carcinoma. Oral Dis. 2011;17:355–61.
67. Desgrosellier JS, Cheresh D a. Integrins in cancer: biological implications and therapeutic opportunities. Nat. Rev. Cancer. 2010;10:9–22.
68. Del Pozo M a, Balasubramanian N, Alderson NB, Kiosses WB, Grande-García A, Anderson RGW, et al. Phospho-caveolin-1 mediates integrin-regulated membrane domain internalization. Nat. Cell Biol. 2005;7:901–8.
69. Fukazawa H, Noguchi K, Masumi A, Murakami Y, Uehara Y. BimEL is an important determinant for induction of anoikis sensitivity by mitogen-activated protein/extracellular signal-regulated kinase kinase inhibitors. Mol. Cancer Ther. 2004;3:1281–8.
70. Akiyama T, Dass CR, Choong PFM. Bim-targeted cancer therapy: a link between drug action and underlying molecular changes. Mol. Cancer Ther. 2009;8:3173–80.
71. Li a. E, Ito H, Rovira II, Kim K-S, Takeda K, Yu Z-Y, et al. A Role for Reactive Oxygen Species in Endothelial Cell Anoikis. Circ. Res. 1999;85:304–10.
72. Fung C, Lock R, Gao S, Salas E, Debnath J. Induction of autophagy during extracellular matrix detachment promotes cell survival. Mol. Biol. Cell. 2008;19:797–806.
73. Luo S, Garcia-Arencibia M, Zhao R, Puri C, Toh PPC, Sadiq O, et al. Bim inhibits autophagy by recruiting Beclin 1 to microtubules. Mol. Cell. 2012;47:359–70.
74. Lock R, Debnath J. Extracellular matrix regulation of autophagy. Curr. Opin. Cell Biol. 2008;20:583–8.
75. Taddei ML, Giannoni E, Fiaschi T, Chiarugi P. Anoikis: an emerging hallmark in health and diseases. J. Pathol. 2012;226:380–93.
76. Weigelt B, Peterse JL, van 't Veer LJ. Breast cancer metastasis: markers and models. Nat. Rev. Cancer. 2005;5:591–602.
77. Nguyen DX, Bos PD, Massagué J. Metastasis: from dissemination to organ-specific colonization. Nat. Rev. Cancer. 2009;9:274–84.
78. Fukazawa H, Mizuno S, Uehara Y. A microplate assay for quantitation of anchorage-independent growth of transformed cells. Anal. Biochem. 1995;228:83–90.
79. Fukazawa H, Noguchi K, Murakami Y, Uehara Y. Mitogen-activated protein/extracellular signal-regulated kinase kinase (MEK) inhibitors restore anoikis sensitivity in human breast cancer cell lines with a constitutively activated extracellular-regulated kinase (ERK) pathway. Mol. Cancer Ther. 2002;1:303–9.
80. Nicoletti I, Migliorati G, Pagliacci MC, Grignani F, Riccardi C. A rapid and simple method for measuring thymocyte apoptosis by propidium iodide staining and flow cytometry. J. Immunol. Methods. 1991;139:271–9.
81. Chunhacha P, Sriuranpong V, Chanvorachote P. Epithelial-mesenchymal transition mediates anoikis resistance and enhances invasion in pleural effusion-derived human lung cancer cells. Oncol. Lett. 2013;5:1043–7.
82. Frisch SM, Ruoslahti E. Integrins and anoikis. Curr. Opin. Cell Biol. 1997;9:701–6.

83. Scaffidi C, Schmitz I, Krammer PH, Peter ME. The role of c-FLIP in modulation of CD95-induced apoptosis. J. Biol. Chem. 1999;274:1541–8.
84. Willis SN, Adams JM. Life in the balance: how BH3-only proteins induce apoptosis. Curr. Opin. Cell Biol. 2005;17:617–25.
85. Terada LS, Nwariaku FE. Escaping Anoikis through ROS: ANGPTL4 controls integrin signaling through Nox1. Cancer Cell. 2011;19:297–9.
86. Hinton a., Sennoune SR, Bond S, Fang M, Reuveni M, Sahagian GG, et al. Function of a Subunit Isoforms of the V-ATPase in pH Homeostasis and in Vitro Invasion of MDA-MB231 Human Breast Cancer Cells. J. Biol. Chem. 2009;284:16400–8.
87. Pérez-Sayáns M, Somoza-Martín JM, Barros-Angueira F, Rey JMG, García-García A. V-ATPase inhibitors and implication in cancer treatment. Cancer Treat. Rev. 2009;35:707–13.
88. Lebreton S, Jaunbergs J, Roth MG, Ferguson D a, De Brabander JK. Evaluating the potential of vacuolar ATPase inhibitors as anticancer agents and multigram synthesis of the potent salicylihalamide analog saliphenylhalamide. Bioorg. Med. Chem. Lett. 2008;18:5879–83.
89. Supino R, Petrangolini G, Pratesi G, Tortoreto M, Favini E, Bo LD, et al. Antimetastatic effect of a small-molecule vacuolar H+-ATPase inhibitor in in vitro and in vivo preclinical studies. J. Pharmacol. Exp. Ther. 2008;324:15–22.
90. Sennoune SR, Martinez-Zaguilan R. Plasmalemmal vacuolar H+-ATPases in angiogenesis, diabetes and cancer. J. Bioenerg. Biomembr. 2007;39:427–33.
91. Han J, Sridevi P, Ramirez M, Ludwig KJ, Wang JYJ. β-Catenin-dependent lysosomal targeting of internalized tumor necrosis factor-α suppresses caspase-8 activation in apoptosis-resistant colon cancer cells. Mol. Biol. Cell. 2013;24:465–73.
92. Hendrix A, Sormunen R, Westbroek W, Lambein K, Denys H, Sys G, et al. Vacuolar H+ ATPase expression and activity is required for Rab27B-dependent invasive growth and metastasis of breast cancer. Int. J. Cancer. 2013;133:843–54.
93. Lee Y-C, Jin J-K, Cheng C-J, Huang C-F, Song JH, Huang M, et al. Targeting constitutively activated β1 integrins inhibits prostate cancer metastasis. Mol. Cancer Res. 2013;11:405–17.
94. Kozik P, Hodson N a, Sahlender D a, Simecek N, Soromani C, Wu J, et al. A human genome-wide screen for regulators of clathrin-coated vesicle formation reveals an unexpected role for the V-ATPase. Nat. Cell Biol. 2013;15:50–60.
95. Arjonen A, Alanko J, Veltel S, Ivaska J. Distinct recycling of active and inactive β1 integrins. Traffic. 2012;13:610–25.
96. Kozik P, Francis RW, Seaman MNJ, Robinson MS. A screen for endocytic motifs. Traffic. 2010;11:843–55.
97. Tawfeek H a W, Abou-Samra AB. Important role for the V-type H(+)-ATPase and the Golgi apparatus in the recycling of PTH/PTHrP receptor. Am. J. Physiol. Endocrinol. Metab. 2004;286:E704–10.
98. Ivaska J. Unanchoring integrins in focal adhesions. Nat. Cell Biol. 2012;14:981–3.
99. Zhong X, Rescorla FJ. Cell surface adhesion molecules and adhesion-initiated signaling: understanding of anoikis resistance mechanisms and therapeutic opportunities. Cell. Signal. 2012;24:393–401.
100. Huttenlocher A, Horwitz AR. Integrins in cell migration. Cold Spring Harb. Perspect. Biol. 2011;3:a005074.
101. Sakamoto S, Schwarze S, Kyprianou N. Anoikis Disruption of Focal Adhesion-Akt Signaling Impairs Renal Cell Carcinoma. Eur. Urol. European Association of Urology; 2011;59:734–44.
102. Frisch SM, Schaller M, Cieply B. Mechanisms that link the oncogenic epithelial-mesenchymal transition to suppression of anoikis. J. Cell Sci. 2013;126:21–9.

103. Tsuji T, Ibaragi S, Hu G. Epithelial-mesenchymal transition and cell cooperativity in metastasis. Cancer Res. 2009;69:7135–9.
104. Blick T, Widodo E, Hugo H, Waltham M, Lenburg ME, Neve RM, et al. Epithelial mesenchymal transition traits in human breast cancer cell lines. Clin. Exp. Metastasis. 2008;25:629–42.
105. Wyllie AH. "Where, O death, is thy sting?" A brief review of apoptosis biology. Mol. Neurobiol. 2010;42:4–9.
106. Marconi A, Atzei P, Panza C, Fila C, Tiberio R, Truzzi F, et al. FLICE/caspase-8 activation triggers anoikis induced by beta1-integrin blockade in human keratinocytes. J. Cell Sci. 2004;117:5815–23.
107. Banno A, Ginsberg MH. Integrin activation. Biochem. Soc. Trans. 2008;36:229–34.
108. Woods NT, Yamaguchi H, Lee FY, Bhalla KN, Wang H-G. Anoikis, initiated by Mcl-1 degradation and Bim induction, is deregulated during oncogenesis. Cancer Res. 2008;67:10744–52.
109. Akiyama T, Dass CR, Choong PFM. Bim-targeted cancer therapy : A link between drug action and underlying molecular changes. Mol. Cancer Ther. 2009;3173–80.
110. Chiarugi P, Giannoni E. Anchorage-dependent cell growth: tyrosine kinases and phosphatases meet redox regulation. Antioxid. Redox Signal. 2005;7:578–92.
111. Zhu P, Tan MJ, Huang R-L, Tan CK, Chong HC, Pal M, et al. Angiopoietin-like 4 protein elevates the prosurvival intracellular O2(-):H2O2 ratio and confers anoikis resistance to tumors. Cancer Cell. 2011;19:401–15.

APPENDIX

6 APPENDIX

6.1 List of Abbreviations

AKT	Protein kinase B
ANOVA	Analysis of variance between groups
ARCH	Archazolid A
ATP	Adenosin-5'-triphosphat
BCA	Bicinchoninic acid
BCL-2	B-cell lymphoma
BIM	Bcl-2 interacting mediator of cell death
BSA	Bovine Serum Albumine
CO	Control
DISC	Death inducing signaling complex
DMEM:F12	Dulbeccos's Modified Eagle's Medium
DMSO	Dimethyl Sulfoxide
ECM	Extracellular matrix
EDTA	Ethylenediaminetetraacetic acid
EGTA	Ethyleneglycoltetraacetic acid
ERK	Extracellular signal-regulated kinase
EtOH	Ethanol
FACS	Fluorescence activated cell sorter
FADD	Fas-associated death domain protein
FAK	Focal adhesion kinase
FCS	Fetal calf serum
FLIP	FLICE-like inhibitory protein
HFS	Hypotonic fluorochrome solution
MAPK	Mitogen activated protein kinase
MEK	Mitogen activated protein kinase kinase
MTOR	mechanistic target of rapamycin
MTT	Thiazolyl Blue Tetrazolium Bromide
NAC	N-Acetyl-L-Cysteine
RAF	Rapidly Accelerated Fibrosarcoma
RAS	Rat sarcoma
ROS	Reactive oxygen species
SDS-PAGE	Sodium dodecyl sulfate – polyacrylamid-gelelectrophorese
SRC	Sarcoma
TRAIL	TNF related apoptosis inducing ligand

6.2 Publications

6.2.1 Original Articles

Schempp, C. M., von Schwarzenberg, K., Schreiner, L., Kubisch, R., Müller, R., Wagner, E., Vollmar, A. M. (2014). **V-ATPase inhibition regulates anoikis resistance and metastasis of cancer cells**. Molecular Cancer Therapeutics. doi:10.1158/1535-7163.MCT-13-0484

Wiedmann, R. M., von Schwarzenberg, K., Palamidessi, A., Schreiner, L., Kubisch, R., Liebl, J., Schempp, C., Trauner, D., Vereb, G., Zahler, S., Wagner, E., Müller, R.,Scita, G., Vollmar, A. M. (2012). **The V-ATPase-inhibitor archazolid abrogates tumor metastasis via inhibition of endocytic activation of the Rho-GTPase Rac1.** Cancer Research, 72(22), 5976–87. doi:10.1158/0008-5472.CAN-12-1772

Kraft, T. E., Parisotto, D., Schempp, C., Efferth, T. (2009). **Fighting cancer with red wine? Molecular mechanisms of resveratrol.** Critical Reviews in Food Science and Nutrition, 49(9), 782–99. doi:10.1080/10408390802248627

6.2.2 Oral Presentations

Schempp, C. M., von Schwarzenberg, K., Schreiner, L., Kubisch, R., Müller, R., Wagner, E., Vollmar, A. M.; **V-ATPase inhibition regulates anoikis resistance and metastasis of cancer cells**; 4th FOR 1406 Meeting, July 16-18, 2013, Saarbrücken, Germany

Schempp, C. M., von Schwarzenberg, K., Schreiner, L., Kubisch, R., Müller, R., Wagner, E., Vollmar, A. M.; **V-ATPase inhibition regulates anoikis resistance and lung metastasis of breast cancer cells**; Retreat Graduate School LSM, May 5-9, 2013, Starnberg, Germany (honored with the price for best talk)

Schempp, C. M., von Schwarzenberg, K., Schreiner, L., Kubisch, R., Müller, R., Wagner, E., Vollmar, A. M.; **Archazolid A induces anoikis in invasive breast cancer cells**; 3rd FOR 1406 Meeting, September16-18, 2012, Starnberg, Germany

6.2.3 Poster Presentations

Schempp, C. M., von Schwarzenberg, K., Schreiner, L., Kubisch, R., Müller, R., Wagner, E., Vollmar, A. M.; **V-ATPase inhibition regulates anoikis resistance and metastasis of cancer cells**; 21st ECDO Euroconference on apoptosis, September 25-28, Paris, France

Schempp, C. M., von Schwarzenberg, K., Schreiner, L., Kubisch, R., Müller, R., Wagner, E., Vollmar, A. M.; **V-ATPase inhibition regulates anoikis resistance and metastasis of cancer cells**; 1st European Conference on Natural Products: Research and Applications, September 22-25, 2013, Frankfurt, Germany

Schempp, C. M., von Schwarzenberg, K., Schreiner, L., Kubisch, R., Müller, R., Wagner, E., Vollmar, A. M.; **Archazolid A Induces Anoikis in Highly Invasive Breast Cancer Cells: a First Report on Underlying Mechanisms**; Natural Anticancer Drugs, June 30 – July 4, 2012, Olomouc, Czech Republic

Schempp, C. M., von Schwarzenberg, K., Schreiner, L., Kubisch, R., Müller, R., Wagner, E., Vollmar, A. M.; **Archazolid A Induces Anoikis in Highly Invasive Breast Cancer Cells: a First Report on Underlying Mechanisms**; Retreat Graduate School LSM, April 25.30, 2012, Spitzingsee, Germany (honored with the poster price)

6.3 Danksagung

Mein allergrößter Dank geht an Frau Prof. Vollmar. Ich möchte Ihnen ganz herzlich dafür danken, dass Sie mir die Chance gegeben haben, meine Doktorarbeit an Ihrem Lehrstuhl anzufertigen, so wie für die sehr gute Betreuung und Unterstützung über die drei Jahre.
Mit Ihrem Enthusiasmus und Ihrer Begeisterung für die Wissenschaft sind Sie für mich ein großes Vorbild. Vielen Dank für die Geduld und das offene Ohr auch in schwierigen persönlichen wie wissenschaftlichen Belangen. Auch für die ermöglichte Teilnahme an Konferenzen, Workshops so wie der LSM, möchte ich Ihnen danken, so wie ein Teil der FOR1406 sein zu können war phantastisch. Das waren allesamt tolle und wertvolle Erfahrungen. Ich hätte mir keine bessere Stelle für meine Doktorarbeit vorstellen können, auch wegen des hervorragenden Klimas im Arbeitskreis.
Ein großer Dank an Prof. Zahler als Zweitprüfer. Insbesondere Ihre „gefürchteten" Kommentare zum Fortschritt meiner Arbeit haben mich sehr motiviert und wichtigen Input für meine Arbeit geliefert. Bei Fragen zu Mikroskopie und Färbetechniken hatten Sie immer die Zeit und Geduld für Diskussion und Verbesserungsvorschlägen, vielen Dank dafür.
Herrn Prof. Wagner und Herrn Prof. Bracher danke ich ganz herzlich für Ihr Interesse an meiner Arbeit als Dritt- und Viertprüfer, so wie Herrn Prof. Frieß und Herrn Prof. Wahl als Fünft- und Sechstprüfer.

Liebe Karin, einen ganz großen Dank für die gute Betreuung in den letzten drei Jahren. Für deine offene Tür, für deinen Input und deine Geduld und Aufmunterungen wenn es mal wieder nicht so gut gelaufen ist. Auch für die guten Gespräche, die nicht unbedingt immer was mit Wissenschaft zu tun haben mussten.
Liebe Lena, vielen Dank für deine Freundschaft. Dass ich eine so gute Freundin in München finden würde, mit der ich 2 Jahre Studium und 3 Jahre Doktorarbeit zusammen durchstehen kann, hätte ich nicht gedacht.
Meinem Lab-buddy Flo möchte ich auch ganz herzlich danken. 3 Jahre in einem Labor schweißen irgendwie zusammen. Danke für die lustige, ernste, aufregende Zeit. Es ist schön, so gute Freunde bei der Doktorarbeit gefunden zu haben.
Liebe Simone, auch dir vielen Dank für so Vieles. Für deine Freundschaft deine direkte Art, dein offenes Ohr und deine viele viele Hilfe.
Liebe Lina, so schön, dass du nach deiner Masterarbeit zu uns gekommen bist, ich hab mich wirklich sehr gefreut. Zusammen mit Katja habt ihr die „Apoptotiker" sehr bereichert und ich habe die Zeit mit euch beiden im Labor sehr genossen.

Liebe Rebekka, so toll dass du noch eine Weile bei uns bleiben konntest und wir die Chance hatten uns richtig kennen zu lernen. Vielen dank für deine Freundschaft, die wir hoffentlich auch in Zukunft pflegen werden.
Lieber Michi, liebe Verena und liebe Sandra. Vielen Dank für die tollen drei Jahre. Wir haben alle zusammen angefangen und dadurch, finde ich, einen besonderen Zusammenhalt und ein gutes Gruppenklima gehabt. Aus der Doktorarbeit mit so vielen neuen guten Freundschaften zu gehen macht mich sehr glücklich. Danke.
Auch allen anderen Mitgliedern des Arbeitskreises möchte ich hiermit aus ganzem Herzen danken. Ich gehe mit einem weinenden und einem lachenden Auge, da ich viele liebe Menschen vermissen werde.
Ein riesiges Dankeschön geht an Benny. Dafür, dass du mich die drei Jahre aufgeheitert, unterstütz, bestärkt und ermutigt hast. Danke einfach dafür, dass du an meiner Seite warst.

Meiner Familie und meinen Freunden möchte ich im Besondere noch danken.
Meinen lieben Freunden, dass Sie immer an mir fest gehalten haben egal ob in Stuttgart oder München und einfach für ihre Freundschaft. Damit meine ich im Besonderen meine Julia, Miri und Mandy in Stuttgart und meine Lena und Micha in München.
Lieber Martin, liebe Christa auch Euch möchte ich aus ganzem Herzen danken für Euer gutes Zureden und Zuhören und Unterstützen. Dafür, dass Ihr immer Zeit und Geduld für mich hattet.
Meinem Papa, meiner Schwester Callo und meinem Bruder Paul danke ich für die immerwährende Unterstützung und Ermutigung, dass Ihr an mich und den Dr. Tini geglaubt habt und dafür, dass ich euch habe und ich auf euch bauen kann.